Available online at www.sciencedirect.com
SCIENCE DIRECT®
PERGAMON
Continental Shelf Research 23 (2003) 457–481
CONTINENTAL SHELF RESEARCH
www.elsevier.com/locate/csr

A time series of benthic flux measurements from Monterey Bay, CA

William Berelson[a,*], Jim McManus[b], Kenneth Coale[c], Ken Johnson[d], David Burdige[e], Tammy Kilgore[a], Debbie Colodner[f], Francisco Chavez[d], Rafael Kudela[g], Joceline Boucher[h]

[a] *Department of Earth Sciences, University of Southern California, Los Angeles, CA 90089, USA*
[b] *College of Ocean and Atmospheric Sciences, Oregon St. University, Corvallis, OR 97331, USA*
[c] *Moss Landing Marine Labs, Moss Landing, CA 95039, USA*
[d] *Monterey Bay Aquarium Research Institute, Moss Landing, CA 95039, USA*
[e] *Department of Earth and Ocean Sciences, Old Dominion University, Norfolk, VA 23529, USA*
[f] *Biosphere, Oracle, AZ 85623, USA*
[g] *Department of Ocean Sciences, UC Santa Cruz, Santa Cruz, CA 95064, USA*
[h] *Ocean Studies Program, Maine Maritime Institute, Castine, ME 04420, USA*

Received 18 May 2001; received in revised form 5 September 2002; accepted 3 December 2002

Abstract

In situ incubation chamber measurements of benthic nutrient recycling rates were made on the Monterey Bay shelf at 100 m during various years and seasons. Variability in nutrient (Si, PO_4^{2+}, NH_3, NO_3^-) and trace metal (Mn, Fe (II), Cu) fluxes correlate with variability in the amount of organic carbon oxidized on the sea floor. Patterns of primary productivity show a mid-year maxima, consistent with the timing of increased rates of benthic C_{org} and opal recycling. High rates of C_{org} rain to the shelf promote nitrate consumption at a rate that equals or exceeds ammonia efflux. Low rates of C_{org} rain promote greater efflux of DIN; thus these margin sediments provide a negative feedback to local productivity cycles. The efflux of iron (II) from shelf sediments is sufficient to support >100% of new production, yet Fe flux is positively correlated with C_{org} recycling which lags the maximum in new production. On account of this time lag, diagenetically recycled Fe is not likely a micro-nutrient trigger of new production, but could serve as a positive feedback. Bio-irrigation rates are seasonally variable by 30% but maximal during the maximum productivity months.

Keywords: Benthic recycling; Monterey Bay; Nutrients; Carbon

1. Introduction

Continental shelves (defined as 30–200 m) represent <10% of global oceanic area, yet primary productivity in this region accounts for 20–40% of global estimates of this parameter (Walsh et al.,

*Corresponding author. Tel.: +1-213-740-5828; fax: +1-213-740-8801.
E-mail address: berelson@earth.usc.edu (W. Berelson).

0278-4343/03/$ - see front matter
doi:10.1016/S0278-4343(03)00009-8

1981; Christensen, 1989). The high rates of primary production and new production over shelves prompted studies examining the export of POC (C_{org}) from margins to deeper water as a potential sink for anthropogenic CO_2 (Walsh, 1991, 1994). Studies of carbon transport off the mid-Atlantic US continental shelf (SEEP studies, Biscaye et al., 1994) and in the Gulf of Maine (Christensen, 1989) indicated that carbon export off shelves may not occur to a great extent, although a recent estimate (Christensen, 1989) of carbon transport off all continental shelves is 0.3 Gt C/yr (0.3×10^{15} g/yr), which is 15–30% of annual oceanic uptake of CO_2 (1–2 Gt C/yr; Siegenthaler and Sarmiento, 1993). Continental shelves, as a repository of buried C_{org} are considered a minor 'player' in global carbon budgets, only 0.07 Gt C/yr are deposited in shelf sediments which are not associated with deltas (Hedges and Keil, 1995).

There is evidence that upwelling-dominated margins do export a considerable fraction of the newly produced C_{org} to sites further offshore and into deeper water; e.g. the Washington Coast (Christensen et al., 1987), and the Monterey Bay region (Pilskaln et al., 1996) and upwelling-dominated shelves may be more important in C_{org} burial budgets than previously considered. Because burial and offshore transport of shelf-derived C_{org} has the potential to provide a significant sink for atmospheric CO_2 and because there are few locations where carbon budgets for an eastern ocean basin shelf have been established, we developed a carbon budget for the shelf off Monterey, California to examine issues of cross shelf transport, diagenesis and burial. This study differs from others because it considers seasonal variability in the carbon budget.

The Monterey Bay shelf underlies a water column in which primary productivity has a regular, seasonal pattern with maximum productivity between April and July and minimum in December–February (Chavez, 1996). Under such forcing, we examine the response of sea floor diagenetic processes in terms of C, N, P, Si, and trace element recycling. The stoichiometry of biogenic matter recycling is investigated as are the transport processes responsible for solute exchange across the sea floor.

1.1. Site description and methods

A site in the south-central portion of Monterey Bay, 36°44.8′N, 121°55.6′W, was visited 7 times between June 1991 and October 1995. This site lies south of Monterey Canyon, on a flat portion of the shelf at water depth of 95–100 m (Fig. 1). The sediments in this region are sandy muds generally dark green colored. Worm tubes and worms are evident in cores as are a few clams and an occasional shelly layer, typically <1 cm thick. During each cruise, one or two benthic landers (Berelson and Hammond, 1986) were deployed within a few hundred meters of each other. A multi-core device (Barnett et al., 1984) was used to retrieve cores and hydrocasts were taken by rosette and CTD.

Each lander has three chambers, which implant in the sediment several hours following lander deployment. As a free-vehicle, the lander is ballasted by lead bricks, which release to allow recovery at the sea surface following buoyant ascent. The three chambers have lids which seal to a silicone gasket under the force of a springed hinge. Following computer command, six 250 (ml samples are withdrawn from the $\sim$7l chambers. The incubation period of 13–36 h was sufficient to generate measurable changes in concentration, but not long enough to produce significant changes in flux. The chamber water was stirred by a paddle rotating at 5–7 rpm. Near the beginning of the incubation, a spike of Cs, Br or both was injected by spring-loaded syringe. The dilution of this spike enabled the determination of chamber volume and was useful as a tracer for chamber water exchange with pore water.

Oxygen uptake was determined by the slope of electrode output vs. time for pulsed electrodes mounted inside each chamber. Electrodes were calibrated to saturated and oxygen-free water before and after use and also calibrated to bottom water oxygen as determined by Winkler analysis of Niskin samples. Nutrient analyses were carried out by standard spectrophotometric techniques (Parsons et al., 1984) after filtration across 0.4 μm

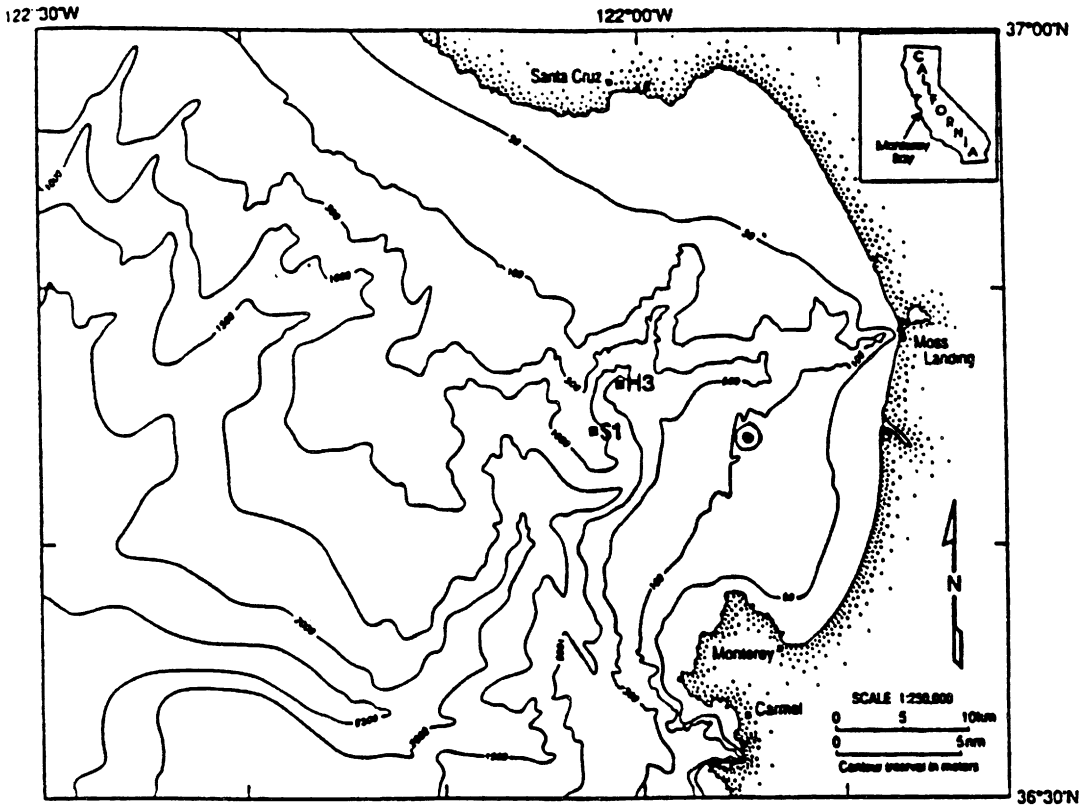

Fig. 1. Site map. Location of benthic station indicated by bullseye. S1 is the sediment trap mooring site and H3 the station where bi-weekly to monthly measurements of primary and new production were conducted. First 4 contour lines are 50, 100, 500, 1000 m.

cellulose filters. Analytical uncertainties for silicate, nitrate + nitrite, phosphate and ammonia were 1%, 2.5%, 2% and 0.2 μM, respectively. Nitrite was determined to contribute <3% to the N + N and hence, hereafter this measure is referred to as nitrate. pH was measured on an unfiltered split of sample using glass electrodes standardized to NBS buffers (±0.02 units). Alkalinity was measured by Gran titration using 5 ml samples (±0.3%). TCO_2 was sometimes measured using a UIC 5012 Coulometer and 4 ml samples (±0.3%), and sometimes calculated from alkalinity and pH (±0.4%). When TCO_2 was determined by both methods, the agreement in flux was better than 30% and we report the mean flux value. pH, ammonia and TCO_2 were measured within 24 h of sample recovery, other nutrients were measured within hours to <10 days.

Carbon oxidation (C_{ox}) and carbonate dissolution are derived parameters, their value defined by the combination of measured TCO_2, alkalinity, nitrate, and ammonia fluxes. The portion of the alkalinity flux attributable to net sulfate reduction was established by determining solid S accumulation rates (0.2 wt% S, unpublished MLML data) and assuming that the S buried is in the form of FeS_2, and that the Fe was originally derived from iron-oxyhydroxides (Hammond et al., 1999). This type of calculation also assumes that the solid S represents a steady-state value and that net sulfate reduction occurs at the same rate during all seasons. The value of 0.5 mmol $S\,m^{-2}\,d^{-1}$ was used for adjustment of alkalinity data and in the derivation of carbonate dissolution rates. In calculating C_{ox} and $CaCO_3$ dissolution rate, we followed the procedure and error analysis described by Hammond et al. (1996) and Berelson

et al. (1998). Briefly, this involves correction of the total alkalinity flux for the ammonia flux, nitrate flux and the alkalinity produced by the net sulfate flux (two equivalents of alkalinity for each mole of sulfate reduced). The alkalinity remaining after these corrections is assumed attributable to $CaCO_3$ dissolution. The value of C_{ox} is derived as the TCO_2 flux minus the contribution from carbonate dissolution.

Radon-222 was measured on 100 ml aliquots of unfiltered sample water utilizing a rapid extraction technique (Berelson et al., 1987). Conductivity was measured ($\pm 0.25\%$) on all sample splits to assure that no de-ionized water mixed with the sample water. Cs was measured by flame emission ($\pm 8\%$) and bromide was measured by colorimetric techniques ($\pm 5\%$) using a method described in the Initial Reports of the Deep-Sea Drilling Project modified by Townsend (1998).

Samples for trace metal analysis were filtered through acid-washed 0.5 μm Millex-LCR filters (Millipore). Samples were analyzed for the trace metals Mn, Cu, and Fe using flow injection analysis with chemiluminescence detection. The Mn analysis is based on the oxidation of 7,7,8,8-tetracyanouinodimethane in an alkaline solution (Chapin et al., 1991). The Cu analysis is based on the oxidation by hydrogen peroxide of a complex formed between Cu and 1,10-phenanthroline (Coale et al., 1992). Iron analysis is based on the reaction of luminol with hydrogen peroxide and Fe(III) in a basic environment (Obata et al., 1993, 1997). Barium was measured by isotope dilution ICP-MS using a Fisons VG PlasmaQuad Plus at Oregon State University (Klinkhammer and Chan, 1990; Klinkhammer and Palmer, 1991).

Fluxes between the sediment and the water incubated in the chambers were determined after correction for dilution which occurs as samples are withdrawn (Table 1). Flux is calculated by linear regression of the corrected chamber data vs. incubation time multiplied by effective chamber height (which varied between 8.5 and 13.9 cm). Bottom water concentration was not used as one of the points regressed against incubation time, although the first sample drawn almost always reproduced the bottom water value to ± 1 analytical s.d. The change in concentration of the solutes as a function of incubation time was plotted and we omitted samples from late in the incubation sequence if the trend looked distinctly non-linear. This could occur if chamber concentration provides a feed-back to flux rates (Bender et al., 1989). No flux was reported if we had fewer than 4 data points. A linear fit to the chamber data presumes a constant flux during the incubation period, an approach adopted by other benthic chamber users (Devol, 1987; Bender et al., 1989; Jahnke, 1990; Sayles et al., 1994). Some samples that may have been contaminated by de-ionized water were not included in the fit and data which appeared spurious were rejected utilizing the criteria described by Hammond et al. (1996). Where there are data from more than one chamber, all the fluxes were averaged under equal weighting to describe the mean flux for a site (Table 2). The uncertainty of this mean was calculated using two formulations: (1) as the standard error of the mean, and (2) as the square root of the sum of the variance of each flux value, divided by the number of flux measurements. We report the larger of these two uncertainties.

Sediment cores were placed in a cold van at in situ temperature (4–8°C) immediately following recovery. The cores were sectioned into depth intervals of 0.5–3 cm under an N_2 atmosphere to minimize oxidation artifacts. Sediment from the center of each section was transferred to centrifuge tubes and capped inside the glove bag. The samples were centrifuged at 6000 rpm for 10–15 min, then pore water was filtered under N_2.

Primary productivity measurements utilized ^{14}C uptake incubations calculated following the procedures described in Chavez et al. (1991). New production values were determined using standard ^{15}N protocol (Dugdale and Wilkerson, 1986). Porosity was measured on sediment samples which were weighed wet and dry and corrected for salt content. Pb-210 was measured by alpha counting and corrected for background Pb-210 by accounting for the activity of Ra-226. Weight % biogenic Si was determined by sequential alkaline leaching with 5% Na_2CO_3 (Conley, 1998). Weight % C_{org} was determined by CNS analyzer (Carlo Erba) corrected for carbonate by analysis with a Coulimetrics analyzer.

Table 1
Flux summary for all chamber deployments at Monterey Bay. Fluxes in mmol $m^{-2} d^{-1}$ except alkalinity (meq $m^{-2} d^{-1}$) and radon (atoms $m^{-2} s^{-1}$). Negative fluxes into the sediments

Cruise/Lander ID/Date	BW O_2 (μM)	Ammonia	Nitrate	Phosphate	Silica	Alkalinity	TCO_2	Oxygen	Radon
CC1-I-R—6/91	132	0.50	−0.70	0.070	7.92	4.62	9.1	−11.1	138
CC1-I-Y		0.83	−0.75	0.075	7.33	4.21	8.6	−10.7	152
CC2-V-B—5/92	142	0.59	−0.60	0.120	7.33	3.06	—	−10.8	251
CC2-V-R		0.60	−0.64	0.093	7.74	6.50	12.1	−8.6	242
CC2-V-Y		0.57	−0.61	0.172	8.63	4.92	11.3	−10.2	266
TS1-VII-B—6/93	101	0.29	−1.18	0.058	5.36	2.21	8.5	−5.0	274
TS1-IV-B		0.78	−0.66	0.031	8.33	4.20	11.5	−7.6	276
TS1-IV-R		0.39	−0.83	0.021	6.81	4.35	8.9	−6.1	291
TS2-IV-B—9/93	135	1.27	−1.04	0.137	11.9	1.61	10.8	−12.0	320
TS2-IV-R		1.56	−0.89	0.109	11.9	2.53	11.0	−10.3	376
TS2-IV-Y		1.06	−0.65	0.108	9.41	4.60	10.7	−8.5	346
TS2-VII-B		0.46	−1.96	0.088	9.54	2.05	12.0	−11.6	205
TS2-VII-R		0.80	−2.08	0.109	10.3	−0.66	8.1	−11.1	167
TS2-VII-Y		0.84	−0.57	0.073	8.01	2.15	10.9	−10.3	170
TS3-IV-B—12/93	185	0.48	0.25	0.107	5.03	4.54	8.4	−9.6	297
TS3-IV-Y		0.12	0.18	0.091	3.06	3.53	6.1	−6.7	127
TS4-IV-B—3/94	133	0.25	−0.55	0.070	4.92	−0.61	4.7	−6.7	147
TS4-IV-R		0.41	−0.02	0.090	5.86	3.12	8.4	−5.8	253
TS4-IV-Y		0.33	−0.34	0.110	5.32	−0.08	4.8	−5.1	292
TS4-VII-B		0.28	0.26	0.117	5.86	2.51	8.1	−6.0	280
TS4-VII-R		0.30	−0.55	0.003	3.41	5.84	8.7	−5.7	134
TS4-VII-Y		0.14	0.80	0.130	4.18	3.40	7.1	−6.4	178
CC3-VII-B—10/95	153	0.48	−0.61	0.250	8.85	7.17	12.4	−13.0	166
CC3-VII-R		0.72	−0.70	0.256	9.93	11.7	17.8	−9.7	211
CC3-VII-Y		0.49	−0.73	0.292	11.4	8.56	13.8	−13.5	265

2. Results

2.1. Chamber data

The change in concentration as a function of incubation time was determined for measurements of ammonia, nitrate, phosphate, dissolved silica, alkalinity, TCO_2, oxygen, radon, copper, manganese, iron (II), and barium. Table 1 contains a summary of nutrient fluxes for all chambers deployed at the Monterey site; Fig. 2 illustrates chamber nutrient data for the CC3 cruise. Individual chamber trace element flux data are given by Kingsley (1999), and McManus et al. (1994). The data presented in Fig. 2 are representative of nutrient flux data; sometimes the chamber data describe a trend that fits a linear function to better than 5%, often the uncertainty in slope is 10–20%. By averaging chamber fluxes, a representative value for flux can be established for each cruise period. Averaging chambers accounts for the heterogeneity in fluxes on a scale length of 0.5 m, the distance between chambers, and 100's m, the distance between landers. The average flux for a particular cruise period as presented in Table 2 takes into account all the chambers deployed during that cruise period.

Oxygen uptake ranged between 5.0 and 13.5 mmol $m^{-2} d^{-1}$, the greatest uptake rate was in October 1995, the lowest in June 1993. TCO_2

Table 2

Cruise ID (# chambers)	Ammonia	Nitrate	Phosphate	Silica	Alkalinity	$\sum CO_2$	Oxygen	Rn
(a) Monterey Bay time series flux summary. Fluxes are mmol/m^{2}d except alkalinity, meq/m^{2}d, and Rn, atoms/m^{2}s.								
CC1 (2)	0.66±0.17	−0.72±0.07	0.073±0.010	7.62±0.77	4.42±0.56	8.86±0.98	−10.91±1.43	145±31
CC2 (3)	0.59±0.03	−0.62±0.04	0.128±0.023	7.90±0.38	4.83±0.99	11.73±1.04	−9.87±1.32	253±22
TS1 (3)	0.49±0.15	−0.89±0.16	0.037±0.011	6.83±0.86	3.59±2.00	9.62±1.41	−6.21±0.74	280±18
TS2 (6)	1.00±0.16	−1.20±0.27	0.104±0.009	10.17±0.62	2.05±0.84	10.57±0.57	−10.64±0.88	264±38
TS3 (2)	0.30±0.18	0.21±0.09	0.099±0.013	4.04±0.99	4.04±1.05	7.26±1.15	−8.14±1.47	212±85
TS4 (6)	0.29±0.05	−0.07±0.22	0.087±0.019	4.93±0.40	2.36±0.98	6.94±0.74	−5.95±0.78	214±28
CC3 (3)	0.56±0.11	−0.68±0.05	0.266±0.024	10.07±0.75	9.13±1.68	14.69±1.94	−12.08±1.52	214±29

(b) Monterey Bay time series flux summary. Fluxes are μmol/m^{2}d.

Cruise ID (# chambers)	Barium	Manganese	Fe (II)	Copper
CC1 (2)	—	9.06±0.95	1.26±0.16	1.46±0.95
CC2 (3)	—	6.02±1.53	3.84±0.56	1.40±0.49
TS1 (3)	1.65±1.22	17.7±7.10	7.01±2.53	1.90±1.09
TS2 (6)	0.82±0.78	11.1±1.50	4.97±1.93	0.15±0.65
TS3 (2)	2.13±0.81	3.00±1.14	2.04±0.58	0.02±0.16
TS4 (6)	2.36±0.86	4.44±0.75	6.34±1.62	0.65±0.42
CC3 (3)	3.26±0.38	17.0±3.45	10.79±3.91	—

flux had a slightly greater range, between 4.7 and 17.8 mmol m^{-2} d^{-1}. However, TCO_2 fluxes were lowest in December 1993 and March 1994, which does not coincide with the period of lowest oxygen uptake. Alkalinity fluxes were mostly out of the sediments (+), but a few fluxes were into the sediments (−) although these fluxes had uncertainties that allow for a zero flux. Individual chamber alkalinity fluxes ranged from −0.7 to 8.6 meq m^{-2} d^{-1}. Ammonia flux was always positive and ranged from 0.1 to 1.6 mmol m^{-2} d^{-1}. The lowest ammonia fluxes occurred during cruises TS3 (December 1993) and TS4 (March 1994). Nitrate flux was almost always into the sediments with a few exceptions; the range in nitrate flux was −2.1–0.3 mmol m^{-2} d^{-1}. The smallest negative and only net positive nitrate flux occurred during cruises TS3 and TS4. Phosphate flux showed the greatest variability both within chambers of a lander and between two lander deployments. There was always a positive flux of phosphate from Monterey Bay sediments, although in one chamber the flux was close to nil. In most chambers the phosphate flux was close to 0.1 and got as high as 0.3 mmol m^{-2} d^{-1}. Dissolved silicate flux was very consistent between chambers and between landers; the range in fluxes was 3.1–11.9 mmol m^{-2} d^{-1}. Dissolved Si fluxes were lowest during TS3 and TS4 cruises and highest during TS2 and CC3 cruises. Radon-222 fluxes varied three-fold, from 130 to 380 atoms m^{-2} s^{-1}.

2.2. Solid phase and pore water data

Down-core changes in porosity, Pb-210 activity, wt% biogenic Si and wt% organic C were measured on cores collected using a multi-corer, a device which assures the collection of the sediment-water interface. Porosity was determined on 9 cores collected during the time-series study; replicate cores from the same cruise period showed very similar down-core structure. Surficial sediments have a porosity of approx. 0.65–0.7 and this value decreases to 0.4–0.5 at 20–25 cm (Fig. 3).

The Pb-210 profile shows a region of quite consistent excess Pb values in the upper 7 cm and a decline in activity below 7 cm (Fig. 3). The change in Pb-210 activity below 7 cm was used to define a linear sediment accumulation rate, 0.25 cm/yr. If sediment mixing occurs below this horizon, this estimate will be an upper limit. However, three other cores were collected from the region near the

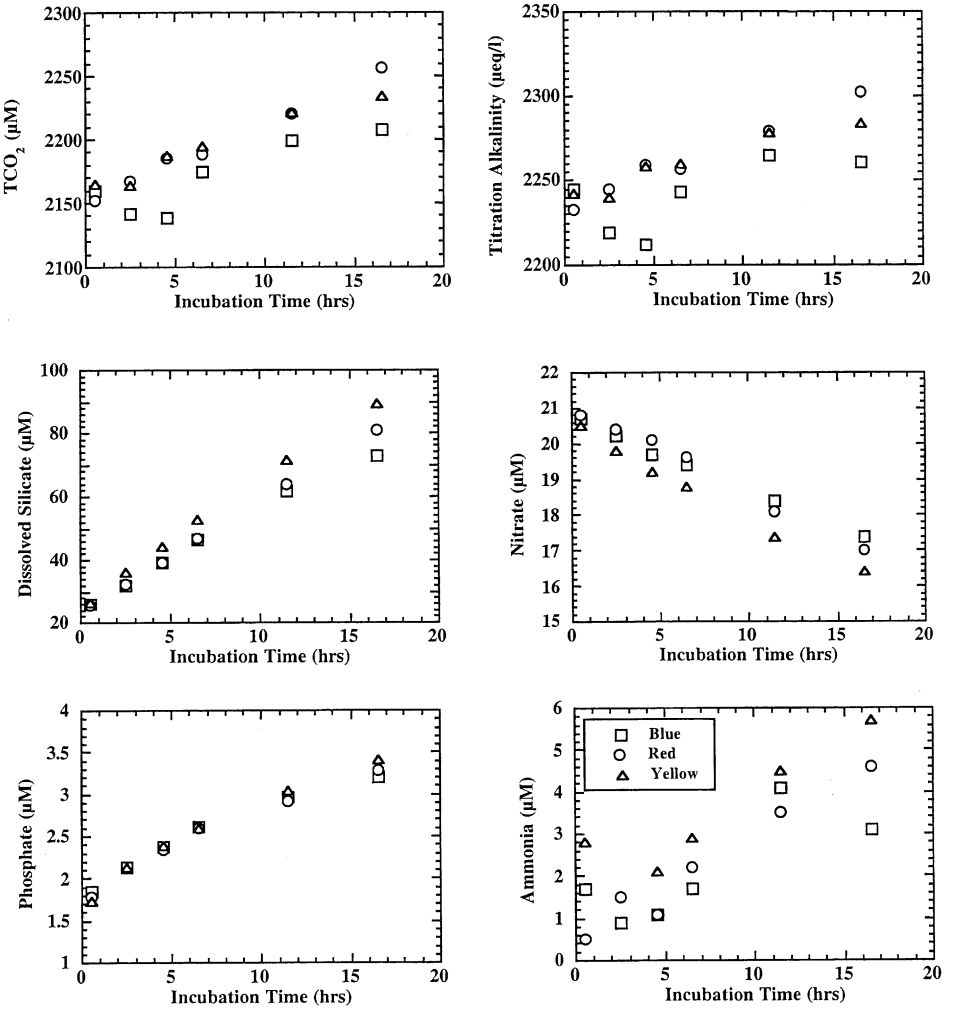

Fig. 2. Chamber data from the CC3 cruise period. Three symbols indicate three chambers on the same lander. Analytical uncertainty is less than the size of the symbols except for TCO_2 ($\pm 9\,\mu M$) and Alkalinity ($\pm 7\,\mu eq/l$).

benthic station and also analyzed for excess Pb-210 (Lewis, 2000). The average from all 4 cores indicate a sediment accumulation rate of 0.20 ± 0.04 cm/yr and this was the value used for accumulation rate calculations.

There is variability in solid phase organic carbon content; wt% fluctuates between 0.2 and 0.5. The profile of biogenic opal shows structure similar to C_{org} and varies between 0.5 and 0.8 wt% Si.

Pore water profiles of dissolved Si (Fig. 4) and nitrate (Fig. 5) are presented from replicate cores representing the cruise periods TS1 through TS4 and CC-3. Bottom water Si concentrations (20–40 μM) are much lower than dissolved Si in pore waters from the upper-most sediment interval (200–500 μM). Pore water profiles show good reproducibility between two multi-core tubes collected during the same deployment, yet profiles vary between cruise periods, as discussed below. All profiles show a tendency for dissolved Si in pore waters to obtain a value of approximately 300 μM at depths below 15 cm. Bottom water nitrate varied between 15 and 30 μM. Pore water nitrate values declined from bottom water to $<2\,\mu M$ within the top 10 cm and fluctuated

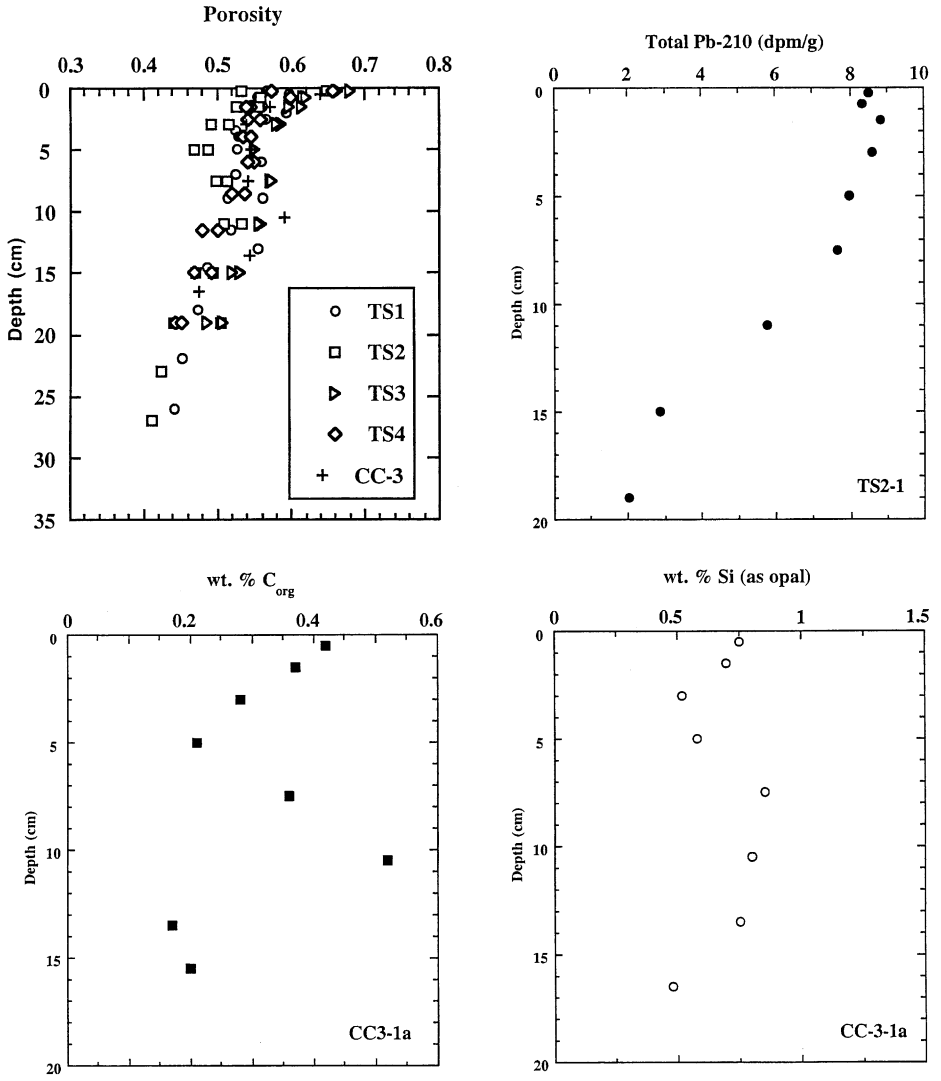

Fig. 3. Sediment profiles of porosity, Pb-210, wt% C_{org} and wt% Si from cores collected in Monterey Bay. Cruises are indicated by the cruise identifier in the bottom right of each plot. Depth intervals were 0.5 cm for the first two points, 1 cm for the next 3 points and 2 cm for each subsequent point, data are plotted at the mid-point of the interval. Ra-226 activity is consistent downcore at 0.1 dpm/g.

between 0 and 2 μM for the rest of the cored interval.

3. Discussion

3.1. Diffusive fluxes vs. chamber fluxes

Transport mechanism is always an important question when studying solute fluxes across the sediment-water interface. At 100 m water depth, it is not well known if fluxes are likely to be controlled by diffusive transport or affected by bio-irrigation. A study from the Washington shelf clearly demonstrated that bio-irrigation can be important at this depth (Archer and Devol, 1992). A comparison of diffusive vs. chamber fluxes for a suite of nutrients and conservative tracers was used to determine if irrigation is important on the Monterey Bay shelf and if irrigation has a seasonally modulated component.

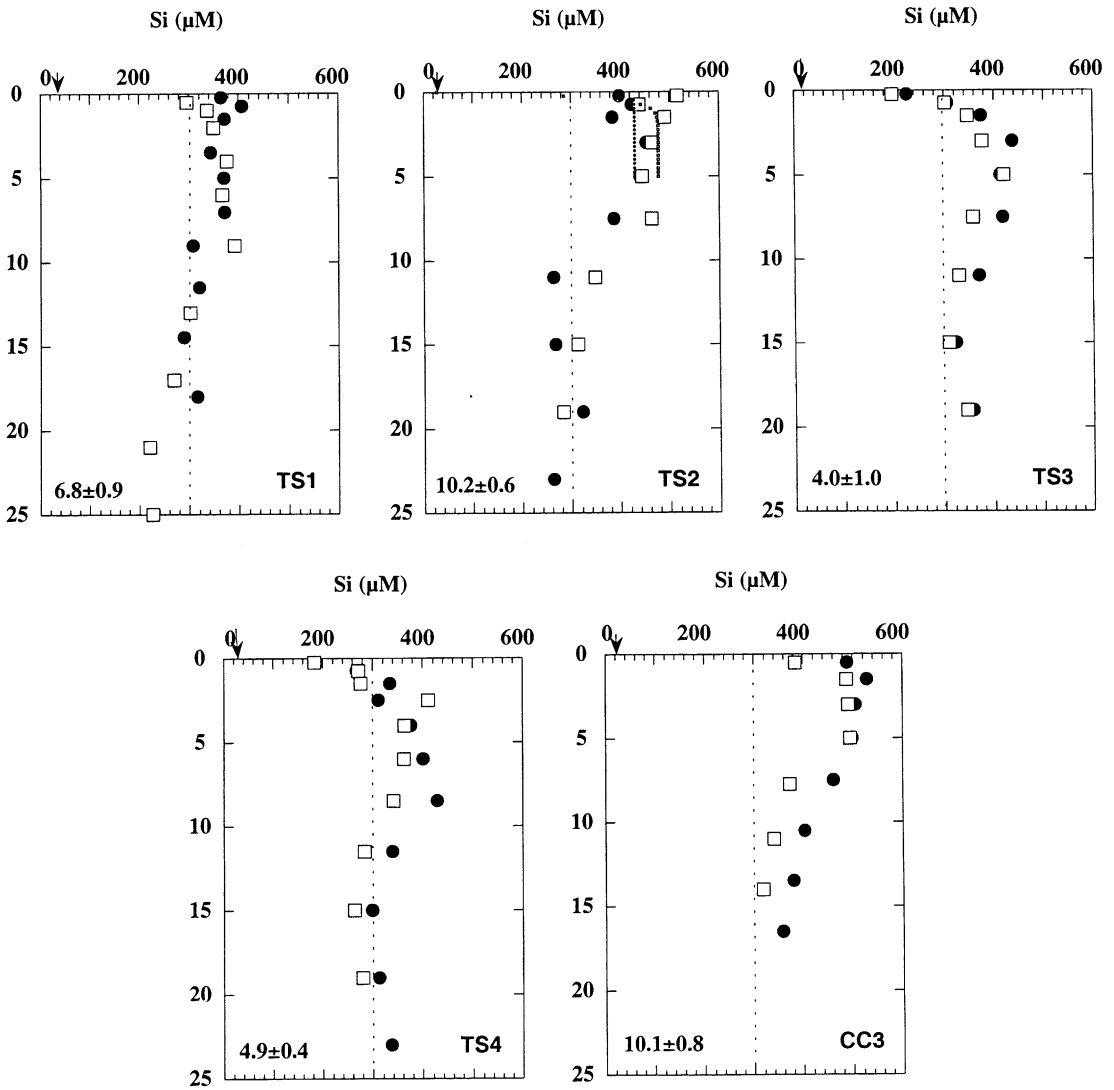

Fig. 4. Pore water profiles of dissolved Si. Two cores were processed during each cruise period and are identified by the different symbols. Arrows on upper axis indicate bottom water values. Numbers in lower left of each panel indicate Si flux determined by chamber measurements (mmol $Si\,m^{-2}\,d^{-1}$). The dashed line at 300 μM provides reference to a concentration that the profiles tend toward at depths >10 cm. Model fits, following Eq. (1), are shown for the data from TS2. Depth scale in cm.

Pore water profiles (Figs. 4 and 5) provide an indication of the gradient in nitrate and dissolved silica (hereafter, silicate) between the overlying water and the upper cm's of the sediment pore waters. The first two pore water sample intervals were from 0 to 0.5 and 0.5 to 1.0 cm, other intervals were 1 or 2 cm integrals. We used the mid-point of these depth intervals as representative of the sample location. The diffusive flux calculation relies on the slope of this gradient at the sediment water interface and the properties which control diffusivity (Reimers et al., 1992). Analytical solutions to concentration vs. depth were determined by fitting profiles of silicate and nitrate for the upper 5–7 cm. The effect of a diffusive boundary layer was ignored in this

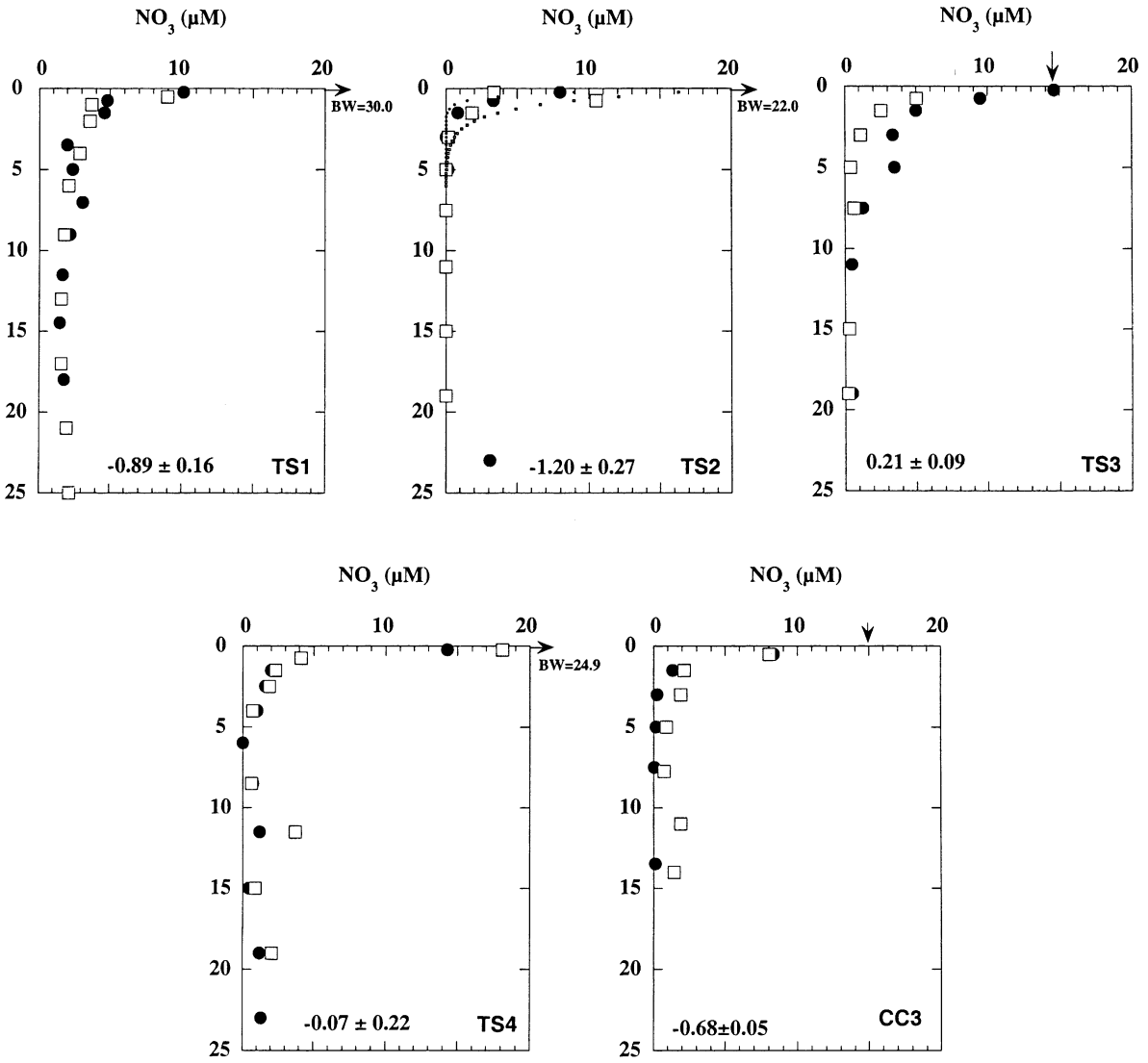

Fig. 5. Pore water profiles of nitrate. Two cores were processed during each cruise period and are identified by the different symbols. Arrows on upper axis indicate bottom water values. Numbers in lower left of each panel indicate nitrate flux determined by chamber measurements (mmol $N\,m^{-2}\,d^{-1}$). Model fits, following Eq. (3), are shown for the data from TS2. Depth scale in cm.

model. The equations were chosen for the quality of their data-fit, not because they represent a fundamental aspect of solute production and transport. Silicate data were fit with the equation:

$$C = m_1 - (m_1 - C_o)\exp(-m_2 z), \quad (1)$$

where C is the pore water silicate concentration, m_1 and m_2 are fitting parameters, C_o is the bottom water concentration of silicate and z is depth in the sediment profile (positive down). This exponential solution does not characterize the deeper part of silicate profiles which often shows a maximum, but this formulation has been used by other modelers to describe silicate profiles in marine sediments (McManus et al., 1995). Diffusive fluxes were derived from Eq. (1) following:

$$\text{Flux} = -\phi D_s \mathrm{d}C/\mathrm{d}z]_0, \quad (2)$$

where ϕ is the sediment porosity for the upper few cm's, D_s is solute diffusivity corrected for temperature and tortuosity (assuming $\theta^{-2} \sim \phi^{1.6}$ after Ullman and Aller, 1982). $dC/dz]_0$ represents the concentration gradient at the sediment-water interface, and is derived from the fit of Eq. (1). The average porosity value for the upper 5 cm of each core was used in the calculation of flux. Two replicate cores were analyzed, hence two estimates of diffusive flux were averaged to produce the flux estimate reported in Table 3.

Nitrate profiles were fit with Eq. (1) and also fit with the equation:

$$C = C_o \exp(-m_3 z). \quad (3)$$

The fluxes derived using either Eq. (1) or Eq. (3) agreed to $\pm 10\%$ and Eq. (3) was chosen as the better fitting expression for estimating nitrate fluxes.

The comparison of chamber and pore water-derived flux estimates indicate that an advective mode of solute transport is important on the Monterey Bay sea floor (Table 3). All the chamber silicate fluxes are greater than the diffusive estimates. The range in Si fluxes between high and low flux periods is 2–3 × for both methods of flux estimation. TS3 and TS4 were time periods when Si flux was low as indicated by both the chamber and pore water data.

The magnitude of nitrate uptake determined by chamber measurements is greater than the diffusive gradient would predict in 3 of 4 time periods suggesting that diffusive gradients also underestimate the rate of nitrate consumption. Generally, nitrate consumption is greatest during time periods TS1, TS2 and CC3 and this is reflected in both the chamber and pore water data.

The disagreement between diffusive flux calculations derived from pore water profile fitting and chamber flux measurements indicates that solute transport during all time periods had an advective component. Chamber fluxes of silicate were enhanced by 2.5–5 times over diffusive fluxes; nitrate uptake was generally greater in the chambers by 2.5–11 times over diffusive estimates. Nitrate and silicate fluxes would not be accurately estimated if only pore water data were available.

3.2. Other evidence of bio-irrigation

The diffusive vs. measured flux results provide evidence that solute transport within Monterey Bay sediments has an advective component (bio-irrigation), and that this process is operative year-round. Two other tracer experiments support this conclusion.

Radon-222 fluxes were determined by chamber measurement and by measurement of radon emanation from Monterey Bay sediments. This comparison has been established as a useful tracer of pore water-overlying water exchange and the enhancement of chamber radon flux over predicted diffusive flux has been cited as evidence of bio-irrigative transport of pore waters (Hammond and Fuller, 1979). Chamber radon flux data is presented in Tables 2 and 3 and although there is a range of a factor of 3 in individual chamber radon flux, there is a seasonal signal in flux; the average radon flux for TS1 and TS2 was 272 ± 11 atoms $m^{-2} s^{-1}$; the average for TS3 and TS4 was 213 ± 1.

Table 3
Comparison of lander chamber fluxes to pore water diffusive fluxes. Fluxes in mmol $m^{-2} d^{-1}$ except radon (atoms $m^{-2} s^{-1}$). Negative fluxes into the sediments

	Dissolved silica		Nitrate		Radon	
Cruise ID	Chamber	Pore water	Chamber	Pore water	Chamber	Sediment
TS1	6.8 ± 0.9	3.6 ± 1.9	-0.89 ± 0.16	-0.32 ± 0.08	280 ± 18	30 ± 8
TS2	10.2 ± 0.6	3.1 ± 0.9	-1.20 ± 0.27	-0.12 ± 0.04	264 ± 38	30 ± 8
TS3	4.0 ± 1.0	1.5 ± 0.1	0.21 ± 0.09	-0.04 ± 0.01	212 ± 85	30 ± 8
TS4	4.9 ± 0.4	1.0 ± 0.2	-0.07 ± 0.22	-0.16 ± 0.08	214 ± 28	30 ± 8
CC3	10.1 ± 0.8	2.7 ± 1.4	-0.68 ± 0.05	-0.06 ± 0.01	214 ± 29	30 ± 8

Not only does radon flux vary seasonally but the chamber flux was significantly greater than the flux predicted from sediment radium measurements and diffusive transport (Townsend, 1998). The diffusive flux of radon from Monterey Bay sediments is only 30 atoms $m^{-2} s^{-1}$, 7–10 times less than chamber flux measurements (Table 3). This significant difference in diffusive flux vs. chamber measured flux is further evidence that advective transport is an important contributor to solute exchange in shelf sediments. The radon flux depends on the characterization of radon emanation from sediments and includes the assumption that radon production rate is constant in the upper cm's of the sediment column. However, this flux comparison is not subject to the same uncertainty as the nutrient flux model; i.e. the uncertainty in whether the pore water concentration gradient very close to the sediment-water interface has been accurately described. Thus, in many ways, a radon flux comparison is a more robust assessment of bio-irrigation intensity and seasonality.

The amount by which the measured radon flux exceeds the diffusive supply of radon may be used to establish an estimate of bio-irrigative pore water transport velocity (Hammond and Fuller, 1979). Although the depth at which bio-irrigation takes place is not known, a lower limit for bio-pumping velocity may be established by assuming that irrigation pumps pore waters with a radon concentration established by the radon emanation rate, approx. 0.11 dpm/cm^3 wet sediment (Townsend, 1998). Applying this model, bio-pumping velocities in Monterey Bay sediments range between 0.9 and 1.2 cm/d for cruise periods TS3 and TS1, respectively. This pumping rate may be compared with pumping velocities determined for sites on the Washington shelf by (a) comparison of chamber oxygen fluxes to diffusive fluxes; 0–10 cm/d (Archer and Devol, 1992) and (b) by modeling sulfate pore water profiles; 2–4 cm/d (Christensen et al., 1984a, b). As noted by Devol and Christensen (1993), various methods of determining irrigation rates yield a range of values which differ by a factor of 5–10 depending on what solute is modeled. Results indicate that the rate of pore water irrigation on the Monterey Bay shelf is similar to irrigation rates determined for the Washington shelf.

Dissolved cesium was used as a purposeful tracer to establish whether bio-irrigation rates varied seasonally. With each deployment, a spike of CsCl was injected inside the chamber to provide chamber water with an initial value of 20–40 ppm Cs, enhanced over the ambient Cs concentration of 0–1 ppm. As the incubation progressed, Cs was lost from the chamber water by diffusion into pore waters, by irrigative advection into pore waters, and by adsorption onto sediment particles (Townsend, 1998). The decline in dissolved Cs from chamber water (Fig. 6) will depend on the processes mentioned above. As an arbitrary fitting parameter, m^3 in Eq. (3) was used to describe this loss rate. For this equation fit, C is normalized to a value of 1 at time = 0 (normalized to the initial Cs concentration in a chamber, C_0) and z represents incubation time. This fitting strategy has been shown to be diagnostic of different rates of bio-irrigation (Berelson et al., 1999). Data from 6 cruises show values of m_3 which vary between -0.00033 and $-0.00066\,min^{-1}$ for all but 2 chambers (CC2-5B and TS3-4Y). If all the chamber fit exponents for a given cruise period are averaged and compared (excepting the two anomalous chambers), the sequence of greater to lesser tracer loss, i.e. advective exchange between chamber water and pore water, would be: TS1 > TS2 > CC3 > TS4. This sequence is consistent with the sequence describing radon flux and consistent with the degree to which chamber nutrient flux is enhanced over sediment diffusive flux. Radon flux and Cs loss-rate experiments provide evidence in support of greater advective exchange during TS1 and TS2 periods relative to TS3 and TS4.

The physical transport of fluid between the overlying water column and the sediment pore water column is mediated by organisms living below and at the sediment-water interface within Monterey Bay. There is sufficient evidence from this setting to suggest that (1) bio-irrigation takes place throughout the annual cycle of high and low productivity, (2) bio-irrigation is greater during the spring–summer–fall months, i.e. the time when more C_{org} is falling to the sea floor, compared to the winter months, (3) bio-irrigation enhances the efflux of silicate and the uptake of nitrate in these shelf sediments.

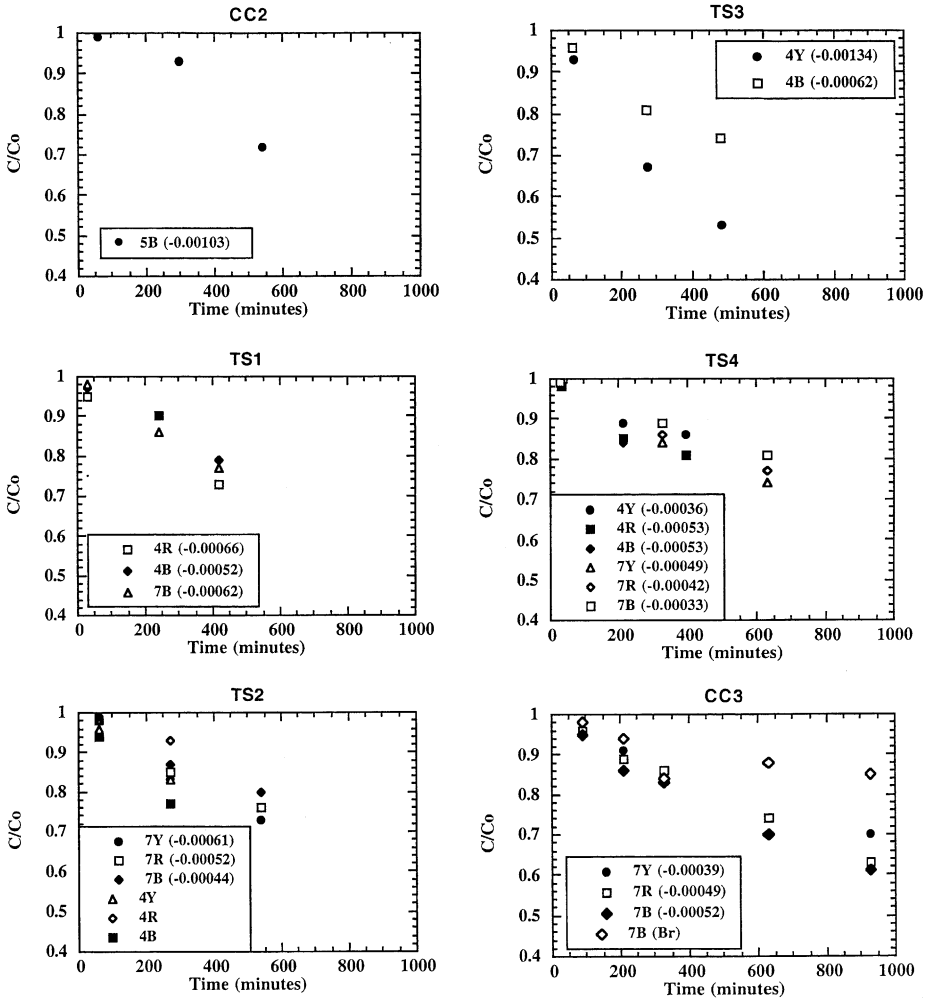

Fig. 6. Cs vs. time plots. *Y*-axis is Cs concentration normalized to initial Cs concentration at time = 0 (when the spike is injected). Values reported in legend box are exponential fit values in min^{-1} (see text). In CC3-7B, Br was also injected with the Cs spike and in this case the *Y*-axis also represents the normalized Br concentration ratio.

3.3. Seasonal variability in fluxes

Primary production in Monterey Bay undergoes a regular seasonal pattern with maximum productivity in April–July and minimum production in December–February. There are year-to-year fluctuations, most notably the suppression of primary productivity during the 1992 El Nino (Kudela and Chavez, 2000). The magnitude and timing of the productivity maximum is more variable than the size and timing of the minima, nonetheless, the annual pattern of primary production is remarkably regular. A 5-year, bi-weekly record defines seasonality in primary productivity (Chavez, 1996) and our multi-year benthic study also shows some seasonality in the pattern of benthic organic carbon oxidation whereby the lowest rates of organic carbon oxidation occur in the winter months (Fig. 7a).

The temporal pattern of fluxes for other biogenic constituents also vary seasonally. Silicate, nitrate and TCO_2 show the strongest variability with large fluxes in June through October and lower fluxes in December and March. There may

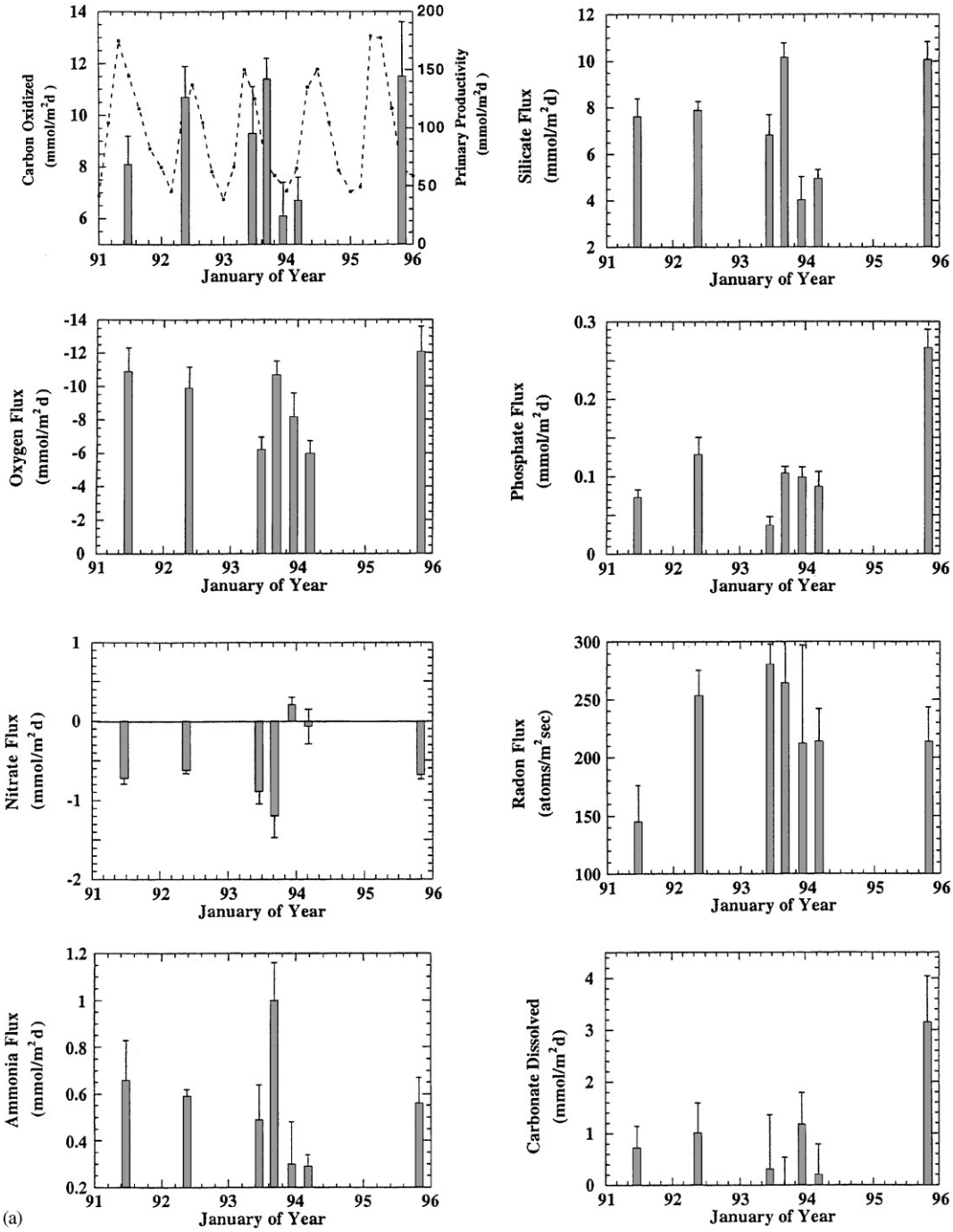

Fig. 7. (a) Plots of nutrient fluxes, C_{ox}, $CaCO_3$ dissolution and primary productivity (dashed line) vs. year. Negative values (oxygen and nitrate) indicate uptake by the sediments. Error bars represent uncertainty in average flux, as discussed in the text. (b) Trace element fluxes vs. year.

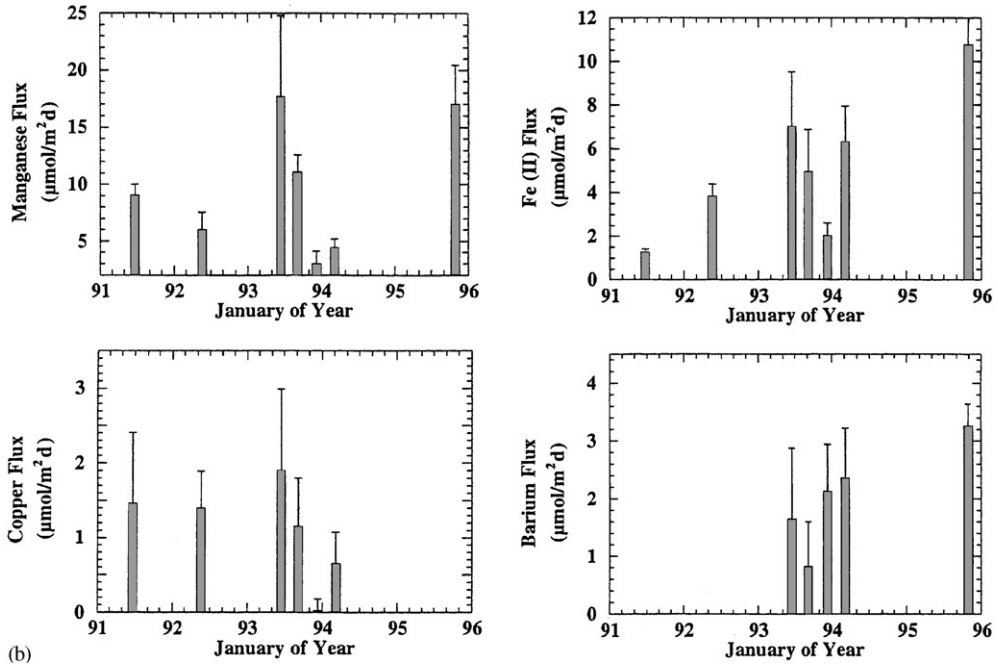

Fig. 7 (*continued*).

be some seasonality in ammonia and radon fluxes, but little seasonality is evident in oxygen or phosphate fluxes. There is no relationship between carbonate dissolution and productivity patterns.

Fluxes of the trace metals Mn, Fe, and Cu also show seasonal variability as fluxes during June and September were on average, greater than fluxes in December and March (Fig. 7b). Barium fluxes showed no systematic relationship to time of year.

The annual pattern of primary productivity is generally symmetric about a maximum in June. This pattern of primary production is similar to the pattern of new production as determined by model and measurement techniques (Kudela and Chavez, 2000), although new production has a more defined peak a little earlier in the year (Fig. 8). The benthic chamber data, collected over a period of 5 years, were reorganized so that all the C_{ox} and Si flux measurements were representative of days within the annual cycle (Fig. 8). Patterns of bio-irrigation intensity were also normalized to an annual cycle and these parameters show a maximum in mid-year, similar to the pattern of C_{org} production, C_{org} oxidation on the sea floor and opal dissolution. To the first order, production of carbon and rain to the sea floor (and diagenesis) are symmetric within the annual cycle. The delivery of C_{org} and biogenic Si to the continental shelf and their regeneration within shelf sediments are tightly coupled.

3.4. Degradation kinetics

The pattern of opal and organic carbon degradation vs. time of year suggest that the degradation rate of these constituents may be fast enough to show seasonality in flux. Published accounts of C_{org} cycling in continental margin sediments indicate values for k_C (the degradation rate constant) that encompass a wide range, but a recent estimate of the C_{org} degradation rate constant on the NE Atlantic continental shelf indicates $k_C \sim 0.1\,d^{-1}$ (Herman et al., 2001). This value is consistent with the degradation rate constant for phytoplankton, bacteria and zooplankton debris (Dauwe et al., 1999). Measurements of opal dissolution rates and standing stocks in water depths between 0 and 300 m from sites in

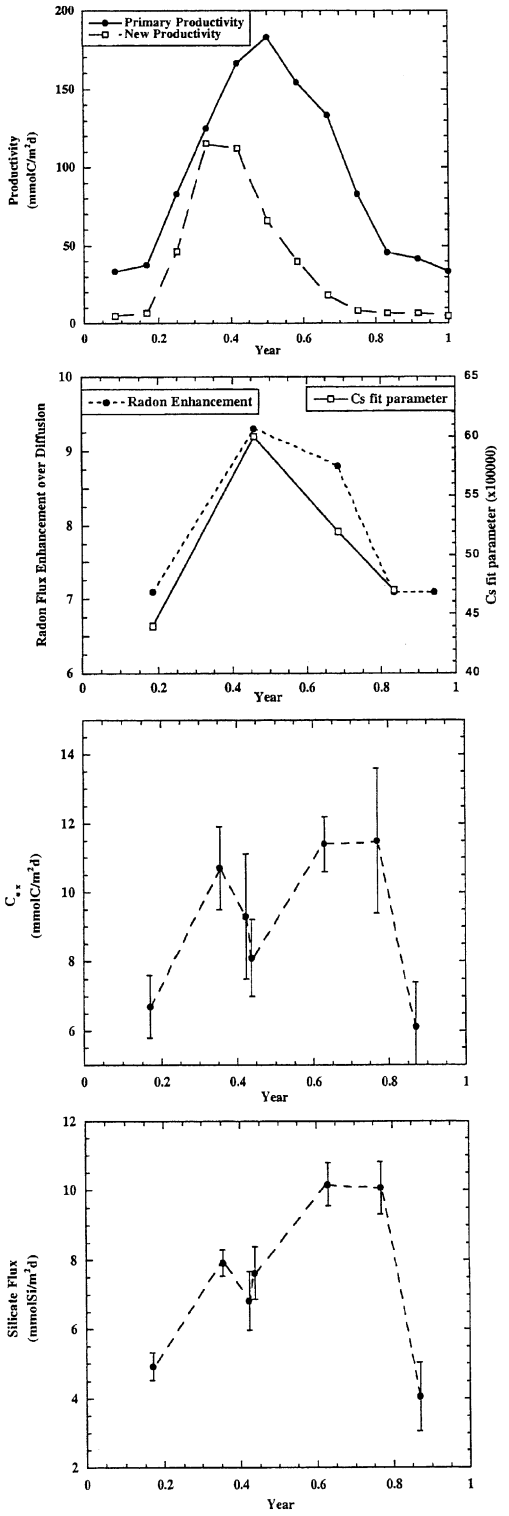

the Southern Ocean yield estimates of k_{Si} that range from 0.003 to 0.14 d^{-1} and average 0.05 d^{-1} (Brzezinski et al., 2001). However, Nelson and Goering (1977) determined much greater values of k_{Si} (0.1–0.5 d^{-1}) for opal in the water column off NW Africa, a coastal site that may be similar to the Monterey Bay site.

We applied a novel approach to assess the values of k_C and k_{Si} which involves modeling the pattern of organic carbon and opal rain as a function of depth through the water column in this region. The pattern of C_{org} rain as a function of depth is described by the relationship (Berelson et al., 1996):

$$F_C = 241z^{(-0.6865)}, \quad (4)$$

where F_C is the rain rate of C_{org} at a given depth horizon (mmol C m^{-2} d^{-1}) and z is depth (> 100 m) in meters. From the same study, the function used to describe opal rain is

$$F_{Si} = 120z^{(-0.5537)}, \quad (5)$$

Rate constants for degradation of C_{org} and dissolution of opal may be derived using the simple formulation (Gnanadesikan, 1999):

$$dF/dz = k(z)F(z)/w, \quad (6)$$

where the change in flux with depth is a function of the rate constant, k (which may be a function of depth) and w, which is the settling velocity of particles. In this formulation, w has units m/d and k has units d^{-1}. For this study, the rate constant was determined for $z = 100$ m and $w = 21$ m/d, a velocity established by observation of particle settling rates in the Monterey Bay region (Pilskaln et al., 1998). Solution to Eq. (6) using Eq. (4) yields $k_C = 0.14\,d^{-1}$ and the solution to Eq. (6)

Fig. 8. (a) The seasonal pattern of average primary and new production in the Monterey Bay region. Primary production pattern from Chavez (1996) and new production pattern from Kudela and Chavez (2000). (b) Seasonal pattern of bio-irrigation as determined using the radon flux enhancement ratio (left axis) and the Cs fitting parameter (right axis). Both measures indicate maximum irrigation rates in the middle of the year. (c) and (d) Pattern of benthic C_{ox} and opal dissolution flux as represented on an annual cycle. Uncertainties in flux represent 1 s.e. of mean flux values.

using Eq. (5) yields $k_{Si} = 0.12\,d^{-1}$. Uncertainty in this modeling approach must take into account the uncertainty in curve fitting the data in Berelson et al. (1996) and uncertainty in estimates of settling velocity (Berelson, 2002); the combined uncertainties in these rate constant estimates is on the order of $\pm 50\%$.

The value of k_C and k_{Si} are consistent with a short lag between production, rain to the sea floor, and diagenetic recycling. Patterns of C_{org} flux as new production, primary production, rain to 100 m and rain to 450 m show patterns that must relate to both physical transport and diagenetic processes (Fig. 9). For example, the difference in magnitude between C_{org} production and delivery to the sea floor at 100 m could represent offshore transport of carbon (Pilskaln et al., 1996) or could indicate intense remineralization between export depths (15–25 m) and shelf depth. Approximately 70% of the annualized average new production is 'lost' and 30% arrives on the shelf. If this material is exported further offshore before sinking, it could contribute to the excess in C_{ox} detected by Jahnke et al. (1990) at depths >4000 m. Between 100 and 450 m, there is a fairly consistent loss of 50% of C_{org} (Fig. 9). While modeling a coastal system in terms of 1-d carbon transport is not completely realistic, the 1-d approach does show how fluxes are linked and also shows how much transport or degradation must be occurring to accommodate a carbon balance.

3.5. Stoichiometry of nutrient and trace element regeneration

Examining solute flux ratios is one method for determining diagenetic stoichiometries and conversely, flux ratios different from certain stoichiometric ratios may be used as evidence of preferential degradation or retention on the solid phase. For example, the molar ratio of organic carbon oxidized to the flux of ammonia + nitrate (DIN) can be viewed as an indicator of DIN reactions within pore water assuming that

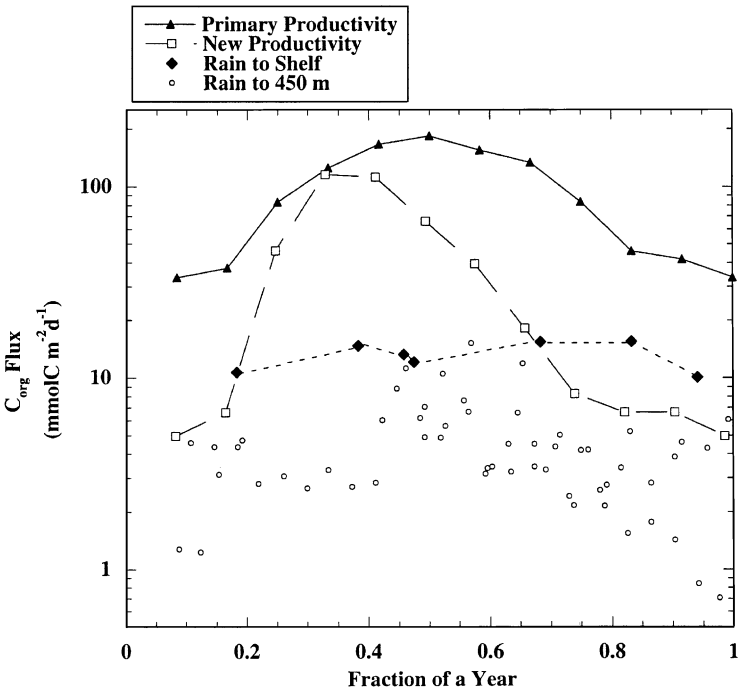

Fig. 9. Annual patterns and rates of C_{org} production, rain to the shelf, and rain to 450 m. Note log scale of flux. The pattern of rain to the shelf is derived by adding the C_{org} burial rate to the seasonal average C_{ox}. C_{org} burial is taken to be constant throughout the year at 4 mmol C $m^{-2}\,d^{-1}$. The rain to 450 m includes trap data from 4 years (Pilskaln et al., 1996).

phytoplankton-derived material is undergoing diagenesis on the sea floor. Following this assumption, the flux ratio expected would be 106 mol organic carbon respired, 16 mol DIN and 1 mol P released. Both the C_{ox} vs. phosphate and C_{ox} vs. DIN flux plots show strong deviations from the predicted Redfield ratio (Fig. 10a). In fact, the most striking relationship observed in flux vs. flux plots appears between carbon oxidized and opal dissolution. The dissolved silicate flux and rate of carbon oxidation follow a slope of approx. 1:1 on a molar basis. There is no readily apparent explanation for this coherence nor this ratio, e.g. diatom-derived material would be expected to have a C_{org}:Si ratio of about 6.6.

Phosphate flux may be related through the Redfield ratio to C_{ox} if there are no further sources or sinks for P. Most P:C_{ox} flux ratios are within 2 s.d. of the Redfield ratio although there is one time when phosphate retention appears to occur and one time when there is an excess flux of P. The very high rate of P release may be generated at high C_{ox} values by the reduction of iron-oxyhydroxides which have scavenged some P (McManus et al., 1997). The period of high P efflux, CC3, was also a period of high Fe (II) flux, supporting this hypothesis.

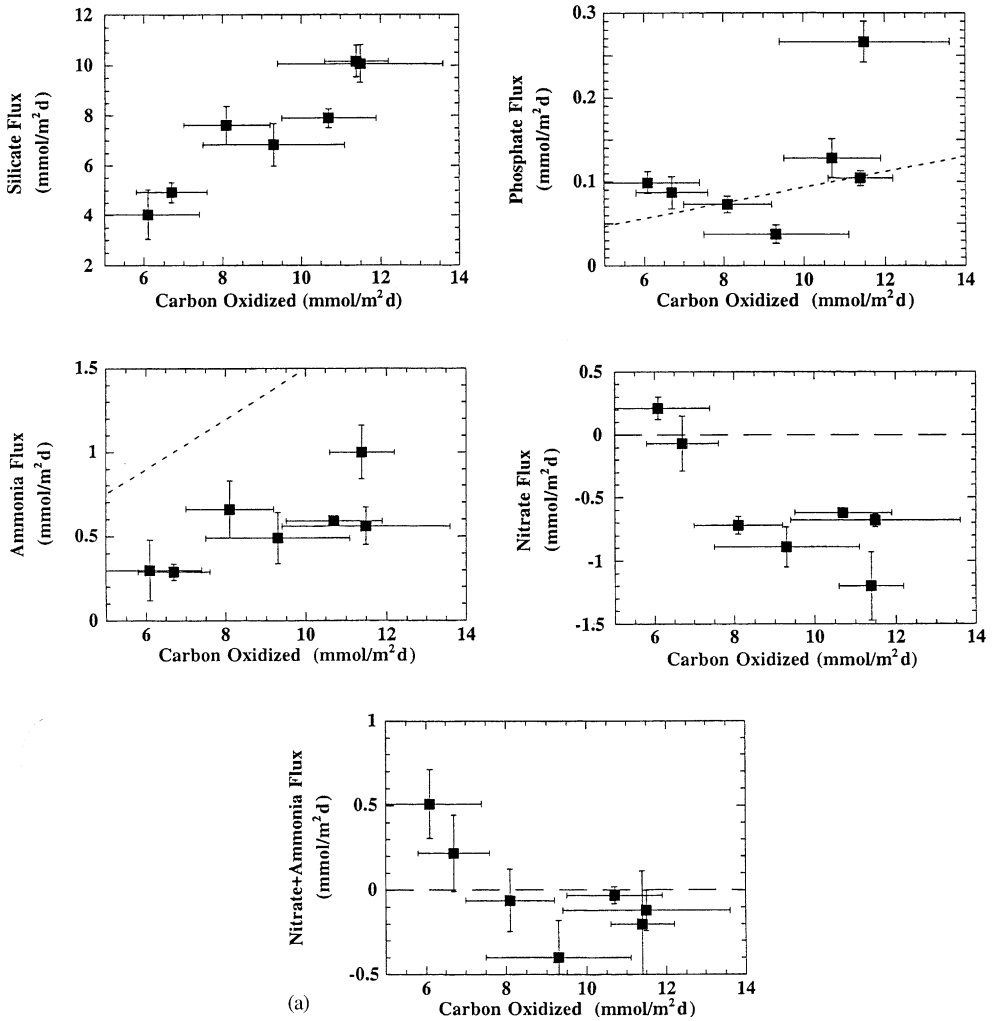

Fig. 10. (a) Nutrient fluxes vs. C_{ox}. Dashed diagonal line represents the Redfield ratio. (b) Trace element fluxes vs. C_{ox}.

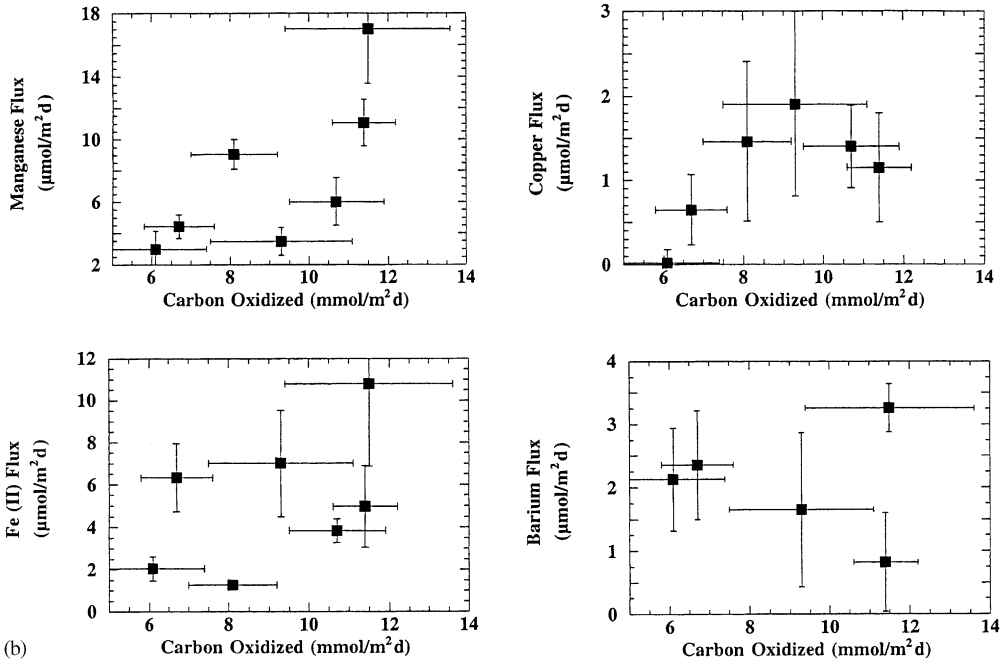

Fig. 10 (*continued*).

The oxidation rate of organic carbon and the release of ammonia to the overlying water show a constant relationship indicating that as greater amounts of organic carbon are remineralized, a similar fraction of the ammonia produced is returned to the overlying water column. Through a range of 2 × in C_{ox}, the efflux of N as ammonia relative to the expected efflux of DIN, remains constant at ~40%. Processes that control the efflux of ammonia must be equally efficient during high and low C_{org} rain rate periods.

Although there was always a positive flux of ammonia from shelf sediments, nitrate flux was only out of the sediments when C_{ox} was low. Nitrate uptake from the overlying water column increased as carbon loading increased (Fig. 10a). During most periods, ammonia was escaping nitrification yet denitrification was drawing nitrate out of the water column. The combined effect of these processes on the N budget was that at low rates of C_{ox} there was a positive return of DIN via recycling at the sediment-water interface, 0.2–0.5 mmol $N\,m^{-2}\,d^{-1}$. However, as C_{ox} exceeds 8 mmol $C\,m^{-2}\,d^{-1}$, nitrate uptake rates and ammonia efflux rates cancel out such that there is no net efflux of DIN.

Previous chamber studies on the central California margin (Berelson et al., 1996) also showed net DIN uptake, even though positive ammonia fluxes were encountered. DIN uptake was maximal between 500 and 1000 m at ~1.0 mmol $N\,m^{-2}\,d^{-1}$. Here we show that shelf sediments, though a source of ammonia, are also a net N sink, especially during times of high production. High rates of C_{org} rain to the shelf promote nitrate consumption at rates that equal or exceed ammonia recycling. Low rates of C_{org} rain promote greater efflux of fixed N, thus these margin sediments provide negative feedback to local productivity cycles.

The trace elements Mn and Fe (II) and Cu show a coherent pattern of flux vs. C_{ox}, yet barium remineralization is not related to organic carbon oxidation (Fig. 10b). The Mn:C_{ox} and Fe:C_{ox} flux ratios (μM:mM) are approx. 1.8 and 1.3, respectively. Within phytoplankton, a typical value of Mn:C_{org} (μM:mM) is 0.044 (Johnson et al., 1996) and Fe:C_{org} (μM:mM) is 0.002–0.05 (Sunda et al.,

1991; Sunda and Huntsman, 1995). Clearly, the Mn and Fe flux relationship to C_{ox} is not reflecting cellular metal burdens which are released as the organic matter is oxidized. Reduction of metal oxides is the likely source of dissolved metal flux and the relationship with carbon oxidation is reflecting the increased reducing state of shelf sediments under greater organic carbon loading.

3.6. Global significance of diagenesis on continental shelves

The uptake of oxygen and exchange of nutrients across continental shelf sediments must be factored into global nutrient and carbon budgets. Fluxes from a variety of shelves, determined primarily with benthic chamber or core incubation techniques are summarized in Table 4. It is interesting to note that, with few exceptions, continental shelf C_{org} remineralization rates are quite similar globally and average about 12 mmol $C\,m^{-2}\,d^{-1}$.

The fluxes determined in this study are not likely representative of most continental shelf environments, yet the range in flux values between eastern boundary-current margins and broad, western ocean basin margins is not great. A few exceptions stand out; e.g. Amazon shelf and San Pedro shelf. The Amazon shelf is a region influenced by high rates of sediment resuspension and a large fraction

Table 4
Summary of fluxes on continental shelves. Fluxes in mmol $m^{-2}d^{-1}$. Negative fluxes into the sediments. The comma separating two values of C_{ox} and C_{org} burial indicate total organic carbon, marine organic carbon. Where no comma is given, the source of the C_{org} is not known but assumed to be marine

Location	Depth range	C_{ox}	Oxygen	Ammonia	Silica	Phosphate	C_{org} burial
Monterey Bay [a]	100	8	−8	0.5	6.5	0.08	4
Washington shelf [b,c,d]	<200	20	−11	0–1.5	4–20	0–0.09	8,4
Amazon shelf [e,f,g]	10–60	47,33	−12	0–1.5	1.3	0–0.09	19,8
Denmark shelf [h]	190	16	−16				
North sea shelf [i]	25–80	11	−11				
China shelf [j]				0.7	2.3		
N. Carolina shelf [k]	30–97	7–15					
Peru shelf [l]	100					0.23	4
E. Canada shelf [m]	90–250		−10				
Alaskan shelf [n]	20–50	9–20	−9–19				
New York shelf [o]	<100	11					1
Maine shelf [p]	32–290	11					1
San Pedro shelf [q]	60	23	−21	3	3.1	0.61	68

[a] This study, flux chambers.
[b] Archer and Devol (1992); flux chambers.
[c] Devol and Christensen (1993); flux chambers.
[d] Christensen et al. (1984); flux chambers.
[e] Aller et al. (1991); core incubations.
[f] Aller et al. (1996); core incubations.
[g] Michaelopolous and Aller (1995); core incubations.
[h] Canfield et al. (1993); core incubations.
[i] Upton et al. (1993); core incubations.
[j] Aller et al. (1995); core incubations.
[k] Rowe et al. (1994); Kemp (1994); core incubations.
[l] Ingall and Jahnke (1994); flux chambers.
[m] Grant et al. (1991); core incubations.
[n] Grebmeier and McRoy (1989); core incubations.
[o] Rowe et al. (1988); core incubations and chambers.
[p] Christensen (1989); pore water modeling.
[q] Berelson et al. (2002); flux chambers.

of the C_{org} remineralized and buried is of terrestrial origin (Aller et al., 1991). The San Pedro Shelf site is anomalous because it may be influenced by input from sewage effluent and recent increases in sediment accumulation due to shoreline erosion (Berelson et al., 2002). These two examples demonstrate that there are shelves with remineralization and C_{org} burial rates that fall well outside the range of values determined for Monterey Bay. There are also shelves with such high sand content that flux measurements are difficult to make (Jahnke et al., 2000) and measurements near large river deltas are underrepresented in this summary.

Organic carbon burial rates are of interest because of the potential impact on global CO_2 budgets. Although carbon recycling rates are fairly uniform between eastern margin and passive margin shelves, C_{org} burial rates are greater on upwelling margins. Assuming a global shelf area (water depths 30–200 m) of $3 \times 10^{13}\,m^2$ and that Monterey Bay is representative of eastern boundary-upwelling shelves, which represent approximately 5% of all continental shelves (Emery, 1968), the burial rate of 4 mmol $C\,m^{-2}\,d^{-1}$ translates into a total burial rate of 0.03×10^{15} gC/yr. If relict sandy shelves represent 70% of all shelves (Emery, 1968) and data from the New York and Maine shelves are representative of these types of margins, a burial rate of 1 mmol $C\,m^{-2}\,d^{-1}$ represents an annual loss term of 0.1×10^{15} gC/yr. Thus, organic carbon burial on upwelling-dominated and relict shelves, by these calculations, total 0.13×10^{15} gC/yr, which is twice the value reported by Hedges and Keil (1995), but still a minor fraction of the oceanic sink for fossil fuel carbon which is $2 \pm 1 \times 10^{15}$ gC/yr (Battle et al., 2000). Finding a way to generalize a few measurements to the global ocean remains a critically important task in assessing C_{org} budgets, yet it is clear that C_{org} burial on upwelling shelves does not provide a significant sink of anthropogenic CO_2 inputs.

The efflux of Fe from the sediments of Monterey Bay may be a source of this trace nutrient to phytoplankton growth. The average Fe flux over a seasonal cycle is 5.1 μmol Fe $m^{-2}\,d^{-1}$. If the Fe requirement of a coastal diatom is 2 μmol Fe:mol C (Sunda et al., 1991), this input of Fe could support diatom growth at a rate of 2550 mmol $C\,m^{-2}\,d^{-1}$. The Fe:C ratio in phytoplankton may be closer to 50 μmol Fe:mol C (Sunda and Huntsman, 1995), in which case the benthic Fe flux could support production of 100 mmol $C\,m^{-2}\,d^{-1}$. New production in this region varies between 10 and 100 mmol $C\,m^{-2}\,d^{-1}$, hence efflux from shelf sediments could supply a significant portion of the Fe required to support coastal production, assuming that only Fe is limiting to new production. However, the Fe flux is positively correlated with C_{org} oxidation rate, which is slightly offset from the timing of maximum new production by a few months. Thus, dissolved Fe from sediment diagenesis is not likely the trigger to new production on the Monterey Bay shelf.

The measurements presented here of nitrate uptake from the water column, termed direct denitrification by Seitzinger and Giblin (1996), occurs at an annually averaged rate of 0.5 mmol $N\,m^{-2}\,d^{-1}$. This rate is 3 times less than the average direct denitrification rate in sediments of the Washington shelf (Devol, 1991), but higher than most of the nitrate uptake rates reported for other shelf environments (Christensen et al., 1987). Again, assuming continental shelves similar to the Monterey shelf represent 5% of the total shelf area, N loss from dissolved nitrate in the water column could occur at a rate of 4 Tg N/yr. If the fluxes measured in this study are representative of the global shelf average, N uptake would occur at a rate of 80 Tg N/yr. Seitzinger and Giblin (1996) estimate global rates of sedimentary denitrification (*N* fixed into phytoplankton, rained to the sediments, released as ammonia, then coupled nitrification and denitrification) at 100 Tg N/yr. Codispoti et al. (2001) offer an updated estimate of global benthic denitrification equal to 300 TgN/yr. Direct denitrification within shelf sediments is an important mechanism of global N removal from the water column.

4. Summary

A time series of benthic flux measurements on the shelf of Monterey Bay (100 m) have been used

to investigate pore water-overlying water transport processes, degradation kinetics, organic matter and trace element diagenetic stoichiometry, and the importance of shelves in global budgets.

(1) The disagreement between diffusive fluxes derived from pore water profile fitting and chamber flux measurements indicates that solute transport during all seasons included an advective component. Chamber fluxes of silicate were enhanced by 2.5–5 times over diffusive fluxes; nitrate uptake was generally greater in the chambers by 2.5–11 times over diffusive estimates. There is sufficient evidence from measurements of chamber fluxes of nutrients, radon and tracer behavior to suggest that (1) bio-irrigation takes place throughout the annual cycle of high and low productivity, and (2) bio-irrigation rates are greater during the spring–summer–fall months by 30%, compared to the winter months.

(2) Nitrate uptake, silicate and TCO_2 fluxes show the strongest seasonal variability with large fluxes in June–October and lower fluxes in December–March. There is some seasonality in ammonia and radon fluxes, but little seasonality is evident in oxygen or phosphate fluxes. There is no relationship between carbonate dissolution and productivity patterns. Fluxes of Mn, Fe, and Cu may be related to seasonal variability as fluxes during June and September were on average, greater than fluxes in December and March. Barium fluxes showed no systematic relationship to time of year. Oxygen uptake is not a master variable in control of the total amount of C_{org} oxidized (C_{ox}), other oxidants become important during the high productivity season.

(3) The seasonal pattern of carbon production, rain to the shelf and rain to 450 m is similar and consistent with a model of particles setting through the water column with a rate constant for opal and C_{org} degradation $\sim 0.1\,d^{-1}$. Over an annual cycle, approx. 30% of the new C_{org} production arrives on the shelf at 100 m. About 50% of the C_{org} arriving at 100 m makes it to 450 m. During high productivity periods, much of the C_{org} produced in the surface ocean may not arrive on the shelf sea floor due to offshore advection or intense water-column recycling.

(4) Although the fraction of ammonia which escapes nitrification is constant as C_{org} rain rate varies, at high rates of C_{org} rain, sedimentary denitrification draws nitrate out of the water column. The combined effect of these processes on the N budget is a positive efflux of DIN (0.2–0.5 mmol $N\,m^{-2}\,d^{-1}$) during the low-upwelling season. However, as C_{ox} exceeds 8 mmol $C\,m^{-2}\,d^{-1}$, nitrate uptake rates and ammonia efflux rates cancel out such that there is no net efflux of DIN. These margin sediments provide a negative feedback to productivity cycles.

Trace elements Mn and Fe (II) show a coherent pattern of flux vs. C_{ox}. The Mn:C_{ox} and Fe:C_{ox} flux ratios (μM:mM) are approx. 1.8 and 1.3, respectively. The efflux of Fe from the sediments of Monterey Bay could be a significant source of this trace nutrient to phytoplankton growth. The average Fe flux over a seasonal cycle is 5.1 μmol $Fe\,m^{-2}\,d^{-1}$ which is sufficient to support C fixation at a rate of 100–2550 mmol $C\,m^{-2}\,d^{-1}$, depending on cellular Fe:C demand. New production in the region varies between 10 and 100 mmol $C\,m^{-2}\,d^{-1}$, hence efflux from shelf sediments could provide > 100% of the Fe required to support coastal production. However, Fe flux is positively correlated with C_{ox}, which is temporally offset from new production. Thus the benthic flux of dissolved Fe does not provide a trigger for new production.

(5) Benthic carbon and nutrient recycling rates do not vary much between upwelling-influenced and trailing-margin shelves. If the Monterey Bay C_{org} burial rate (4 mmol $C\,m^{-2}\,d^{-1}$) is representative of 5% of global continental shelves and the burial rate of 1 mmol $C\,m^{-2}\,d^{-1}$ is representative of relict shelves which occupy 70% of global shelf area, the total burial rate would be 130×10^{12} gC/yr, which is twice the value reported by Hedges and Keil (1995) but still a small fraction of the

oceanic burden of anthropogenic C loading. Assuming that Monterey Bay is representative of upwelling margins, N loss directly from the water column could occur at a rate of 4 Tg N/yr. If the nitrate uptake rate for Monterey Bay is close to the global shelf average, denitrification would account for N loss of 80 Tg N/yr.

References

Aller, R.C., Aller, J.Y., Blair, N.E., Mackin, J.E., Rude, P.D., Stupakoff, I., Patchineelam, S., Boehme, S.E., Knoppers, B., 1991. Biogeochemical processes in amazon shelf sediments. Oceanography 4, 27–32.

Aller, R.C., Mackin, J.E., Ullman, W.J., Hou, W.C., Min, T.S., Cai, J.J., Nian, S.U., Zhen, H.J., 1995. Early chemical diagenesis, sediment-water solute exchange, and storage of reactive organic matter near the mouth of the Changjiang, East China Sea. Continental Shelf Research 4, 227–251.

Aller, R.C., Blair, N.E., Xia, Q., Rude, P.D., 1996. Remineralization rates, recycling, and storage of carbon in Amazon shelf sediments. Continental Shelf Research 16, 753–786.

Archer, D., Devol, A., 1992. Benthic oxygen fluxes on the Washington shelf and slope: a comparison of in situ microelectrode and chamber flux measurements. Limnology and Oceanography 37, 614–629.

Barnett, P.R.O., Watson, J., Connelly, D., 1984. A multiple corer for taking virtually undisturbed samples from shelf, bathyal, and abyssal sediments. Oceanologica Acta 7, 399–408.

Battle, M., Bender, M.L., Taus, P.P., White, J.W.C., Ellis, J.T., Conway, T., Francey, R.J., 2000. Global carbon sinks and their variability inferred from atmospheric O_2 and $\delta^{13}C$ Science 287, 2467–2470.

Bender, M., Jahnke, R., Weiss, R., Martin, W., Heggie, D.T., Orchardo, J., Sowers, T., 1989. Organic carbon oxidation and benthic nitrogen and silica dynamics in San Clemente Basin, a continental borderland site. Geochimica Cosmochimica Acta 53, 685–698.

Berelson, W., 2002. Particle settling rates increase with depth in the ocean. Deep-Sea Research 49, 237–251.

Berelson, W.M., Hammond, D.E., 1986. The calibration of a new free vehicle benthic flux chamber for use in the Deep-Sea. Deep-Sea Research 33, 139–1454.

Berelson, W.M., Hammond, D.E., Eaton, A. 1987. A technique for the rapid extraction of radon-222 from water samples and a case study. In: Graves, B. (Ed.), Radon in Groundwater. National Water Well Association, pp. 271–281.

Berelson, W., McManus, J., Coale, K., Johnson, K., Kilgore, T., Burdige, D., Pilskaln, C., 1996. Biogenic matter diagenesis on the sea floor: a comparison between two continental margin transects. Journal of Marine Research 54, 731–762.

Berelson, W., Heggie, D., Longmore, A., Kilgore, T., Nicholson, G., Skyring, G., 1998. Benthic nutrient recycling in Port Phillip Bay, Australia. Estuarine, Coastal and Shelf Science 46, 917–934.

Berelson, W., Townsend, T., Heggie, D., Ford, P., Longmore, A., Skyring, G., Kilgore, T., Nicholson, G., 1999. Modeling bioirrigation rates in sediments of Port Phillip Bay. Marine and Freshwater Research 50, 573–579.

Berelson, W., Johnson, K., Coale, K., Li, H-C., 2002. Organic matter diagenesis in the sediments of the San Pedro shelf along a transect affected by sewage effluent. Continental Shelf Research 22, 1101–1115.

Biscaye, P.E., Flagg, C.N., Falkowski, P.G., 1994. The shelf edge processes experiment, SEEP-II: an introduction to hypotheses, results and conclusions. Deep-Sea Research 41, 231–252.

Brzezinski, M.A., Nelson, D.M., Franck, V.M., Sigmon, D.E., 2001. Silicon dynamics within an intense open-ocean diatom bloom in the Pacific sector of the Southern Ocean. Deep-Sea Research II 48, 3997–4018.

Canfield, D.E., Jorgensen, B.B., Fossing, H., Glud, R., Gundersen, J., Ramsing, N.B., Thamdrup, B., Hansen, J.W., Nielsen, L.P., Hall, P.O., 1993. Pathways of organic carbon oxidation in three continental margin sediments. Marine Chemistry 113, 27–40.

Chapin, T.P., Johnson, K.S., Coale, K.H., 1991. Rapid determination of manganese in seawater by flow injection analysis with chemiluminescence detection. Analytica Chimica Acta 249, 469–478.

Chavez, F.P., 1996. Forcing and biological impact of onset of the 1992 El Nino in central California. Geophysical Research Letters 23, 265–268.

Chavez, F.P., Jannasch, H.W., Johnson, K.S., Sakamoto, C.M., Friederich, C.E., Thurmond, G.D., Herlien, R.A., Codispoti, L.A., 1991. The MBARI program for obtaining real time measurements in Monterey Bay. Proceedings Oceans 91 (1), 327–333.

Christensen, J.P., 1989. Sulfate reduction and carbon oxidation rates in continental shelf sediments, an examination of offshelf carbon transport. Continental Shelf Research 9, 223–246.

Christensen, J.P., Devol, A.H., Smethie, W.M., 1984. Biological enhancement of solute exchange between sediments and bottom water on the Washington continental shelf. Continental Shelf Research 3, 9–23.

Christensen, J.P., Smethie, W.M., Devol, A.H., 1984. Benthic nutrient regeneration and denitrification on the Washington continental shelf. Deep-Sea Research 34, 1027–1047.

Christensen, J.P., Murray, J.W., Devol, A.H., Codispoti, L.A., 1987. Denitrification in continental shelf sediments has major impact on the oceanic nitrogen budget. Global Biogeochemical Cycles 1 (2), 97–116.

Coale, K.H., Johnson, K.S., Stout, P.M., Sakamoto, C.M., 1992. Determination of copper in sea water using a flow-injection method with chemiluminescence detection. Analytica Chimica Acta 266, 345–351.

Codispoti, L.A., Brandes, J.A., Christensen, J.P., Devol, A.H., Naqvi, S.W.A., Paerl, H.W., Yoshinari, T., 2001. The oceanic fixed nitrogen and nitrous oxide budgets: moving targets as we enter the anthropocene? Scientia Marina 65, 85–105.

Conley, D.J., 1998. An interlaboratory comparison for the measurement of biogenic silica in sediments. Marine Chemistry 63, 39–48.

Dauwee, B., Middelburg, J., Herman, P.M.J., Heip, C.H.R., 1999. Linking diagentic alteration of amino acids and bulk organic matter reactivity. Limnology and Oceanography 44, 1809–1814.

Devol, A., 1987. Verification of flux measurements made with in situ benthic chambers. Deep-Sea Research 34, 1007–1026.

Devol, A., 1991. Direct measurement of nitrogen gas fluxes from continental shelf sediments. Nature 349, 319–321.

Devol, A.H., Christensen, J.P., 1993. Benthic fluxes and nitrogen cycling in sediments of the continental margin of the eastern N. Pacific. Journal of Marine Research 51, 345–372.

Dugdale, R.C., Wilkerson, F.P., 1986. The use of ^{15}N to measure nitrogen uptake in eutrophic oceans; experimental considerations. Limnology and Oceanography 31, 673–689.

Emery, K.O., 1968. Relict sediments on continental shelves of world. A.A.P.G. 52, 445–464.

Gnanadesikan, A., 1999. A global model of silicon cycling: sensitivity to eddy parameterization and dissolution. Global Biogeochemical Cycles 13, 199–220.

Grant, J., Emerson, C.W., Hargrave, B.T., Shortle, J.L., 1991. Benthic oxygen consumption on continental shelves off Eastern Canada. Continental Shelf Research 11, 1083–1097.

Grebmeier, J.M., McRoy, C.P., 1989. Pelagic-benthic coupling on the shelf of the northern Bering and Chuckchi seas. III. Benthic food supply and carbon cycling. Marine Ecology Progress Series 53, 79–91.

Hammond, D.E., Fuller, C., 1979. The use of radon-222 to estimate benthic exchange and atmospheric exchange rates in San Francisco Bay. In: San Francisco Bay: The Urbanized Estuary (Pacific Division of the AAAS), pp. 213–230.

Hammond, D.E., Giordani, P., Berelson, W., Poletti, R., 1999. Diagenesis of carbon and nutrients in sediments of the Northern Adriatic Sea. Marine Chemistry 66, 53–79.

Hammond, D.E., McManus, J., Berelson, W., Kilgore, T., Pope, R., 1996. Early diagenesis of organic carbon in the equatorial Pacific: rates and kinetics. Deep-Sea Research 43, 1365–1412.

Hedges, J.I., Keil, R.G., 1995. Sedimentary organic matter preservation: an assessment and speculative synthesis. Marine Chemistry 49, 81–115.

Herman, P.M.J., Soetaert, K., Middelburg, J.J., Heip, C.H.R., Lohse, L., Epping, E., Helder, W., Antia, A., Peinert, R., 2001. The seafloor as the ultimate sediment trap—using sediment properties to constrain benthic-pelagic exchange processes at the Goban Spur. Deep-Sea Research II 48, 3245–3264.

Ingall, E., Jahnke, R., 1994. Evidence for enhanced phosphorus regeneration from marine sediments overlain by oxygen depleted waters. Geochimica Cosmochimica Acta 58, 2571–2575.

Jahnke, R.A., 1990. Early diagenesis and recycling of biogenic debris at the sea floor. Santa Monica Basin, California. Journal of Marine Research 48, 413–438.

Jahnke, R.A., Reimers, C.E., Craven, D.B., 1990. Intensification of recycling of organic matter at the sea floor near ocean margins. Nature 348, 50–54.

Jahnke, R.A., Nelson, J.R., Marinelli, R.L., Eckman, J.E., 2000. Benthic flux of biogenic elements on the southeastern US continental shelf: influence of pore water advective transport and benthic microalgae. Continental Shelf Research 20, 109–127.

Johnson, K.S., Coale, K.H., Berelson, W.M., Gordon, R.M., 1996. On the formation of the manganese maximum in the oxygen minimum. Geochimica Cosmochimica Acta 60, 1291–1299.

Kemp, P.F., 1994. Microbial carbon utilization on the continental shelf and slope during the SEEP-II experiment. Deep-Sea Research 41, 563–582.

Kingsley, E.S., 1999. Estimating trace element fluxes from continental margin sediments: a comparison of three methods. MS Thesis, San Jose State University, 131pp.

Klinkhammer, G.P., Chan, L.H., 1990. Determination of barium in marine waters by isotope dilution inductively coupled plasma mass spectrometry. Analytica Chimica Acta 232, 323–329.

Klinkhammer, G.P., Palmer, .M.R., 1991. Uranium in the oceans: where it goes and why. Geochimica Cosmochimica Acta 55, 1799–1806.

Kudela, R.M., Chavez, F.P., 2000. Modeling the impact of the 1992 El Nino on new production in Monterey Bay, CA. Deep-Sea Research 47, 1055–1076.

Lewis, R.C., 2000. Accumulation rate and mixing of shelf sediments in the Monterey Bay National Marine Sanctuary. MS Thesis, Moss Landing Marine Laboratories.

McManus, J., Berelson, W., Klinkhammer, G., Kilgore, T., Hammond, D., 1994. Remobilization of barium in continental margin sediments. Geochimica Cosmochimica Acta 58, 4899–4907.

McManus, J., Berelson, W.M., Hammond, D.E., Kilgore, T.E., DeMaster, D.J., Ragueneau, O.G., Collier, R., 1995. Early diagenesis of biogenic opal: dissolution rates, kinetics, and paleoceanographic implications. Deep-Sea Research 42, 871–903.

McManus, J., Berelson, W.M., Coale, K.H., Johnson, K.S., Kilgore, T., 1997. Phosphorus regeneration in continental margin sediments. Geochimica Cosmochimica Acta 61, 2891–2907.

Michalopoulos, P., Aller, R.C., 1995. Rapid clay mineral formation in Amazon delta sediments: reverse weathering and oceanic elemental cycles. Science 270, 614–617.

Nelson, D.M., Goering, J.J., 1977. Near-surface silica dissolution in the upwelling region off NW Africa. Deep-Sea Research 24, 65–73.

Obata, H., Karatani, H., Nakayma, E., 1993. Automated determination of iron in seawater by chelating resin concentration and chemiluminescence detection. Analytical Chemistry 65, 1524–1528.

Obata, H., Karatani, H., Matsui, M., Nakayma, E., 1997. Fundamental studies for chemical speciation of iron in seawater with an improved analytical method. Marine Chemistry 56, 97–106.

Parsons, T.R., Maita, Y., Lalli, C.M., 1984. A manual of chemical and biological methods for seawater analysis. Pergamon Press, Oxford, 173pp.

Pilskaln, C.H., Paduan, J.B., Chavez, F.P., Anderson, R.Y., Berelson, W.M., 1996. Carbon export and regeneration in the coastal upwelling system of Monterey Bay, central California. Journal Marine Research 54, 1149–1178.

Pilskaln, C.H., Lehmann, C., Paduan, J.B., Silver, M.W., 1998. Spatial and temporal dynamics in marine aggregate abundance, sinking rate and flux: Monterey Bay, central California. Deep-Sea Research 45, 1803–1837.

Reimers, C.E., Jahnke, R.A., McCorkle, D.C., 1992. Carbon fluxes and burial rates over the continental slope and rise off central California with implications for the global carbon cycle. Global Biogeochemical Cycles 6, 199–224.

Rowe, G.T., Theroux, R., Phoel, W., Quinby, H., Wilke, R., Koschoreck, D., Whitledge, T.E., Falkowski, P.G., Fray, C., 1988. Benthic carbon budgets for the continental shelf south of New England. Continental Shelf Research 8, 511–527.

Rowe, G.T., Boland, G.S., Phoel, W.C., Anderson, R.F., Biscaye, P.E., 1994. Deep-sea floor respiration as an indication of lateral input of biogenic detritus from continental margins. Deep-Sea Research 41, 657–668.

Sayles, F.L., Martin, W.R., Deuser, W.G., 1994. Response of benthic oxygen demand to particulate organic carbon supply in the deep sea near Bermuda. Nature 371 (6499), 686–689.

Seitzinger, S.P., Giblin, A.E., 1996. Estimating denitrification in North Atlantic continental shelf sediments. Biogeochemistry 35, 235–260.

Siegenthaler, U., Sarmiento, J.L., 1993. Atmospheric carbon dioxide and the ocean. Nature 365, 119–125.

Sunda, W.G., Swift, D.G., Huntsman, S.A., 1991. Low iron requirement for growth in oceanic phytoplankton. Nature 351, 55–57.

Sunda, W.G., Huntsman, S.A., 1995. Iron uptake and growth limitation in oceanic and coastal phytoplankton. Marine Chemistry 50, 189–206.

Townsend, T.H., 1998. Numerical simulations of tracer loss from benthic chambers: An investigation of bio-irrigation rates and patterns in marine sediments. MS Thesis, USC, 156pp.

Ullman, W.J., Aller, R.C., 1982. Diffusion coefficients in nearshore marine sediments. Limnology and Oceanography 27, 552–556.

Upton, A.C., Nedwell, D.B., Parkes, R.J., Harvey, S.M., 1993. Seasonal benthic microbial activity in the southern North Sea; oxygen uptake and sulfate reduction. Marine Ecological Progress Series 101, 273–281.

Walsh, J.J., 1991. Importance of continental margins in the marine biogeochemical cycling of carbon and nitrogen. Nature 350, 53–55.

Walsh, J.J., 1994. Particle export at Cape Hatteras. Deep-Sea Research 41, 603–628.

Walsh, J.J., Rowe, G.T., Iverson, R.L., McRoy, C.P., 1981. Biological export of shelf carbon is a sink of the global CO_2 cycle. Nature 291, 196–201.